



protons and helium in cosmic rays results from AMS



Nicola Tomassetti
LPSC/CNRS – Grenoble, France
on behalf of the AMS Collaboration

*Solar Energetic Particles, Solar Modulation and Space Radiation
New Opportunities in the AMS-02 Era*

October 18 - 23, 2015 – Honolulu, Hawaii, USA

The AMS Project



Particle physics detector for high precision CR measurements at TeV energy

Physics goals

- ✓ Antimatter search ($|Z|>1$ anti-nuclei)
- ✓ Dark Matter (light anti-matter & γ -rays)
- ✓ Exotic signals?
- ✓ **GCR astrophysics & γ -rays**
- ✓ **Heliophysics (long-term modulation & SEP)**
- ✓ Magnetospheric physics & space radiation studies



How it will fulfill these goals?

- **Large collaboration: 16 Countries, 60 Institutes and ~500+ Physicists**
- **Same concept (precision & capability) as the large state-of-the-art HEP detectors [but: fitting into the space shuttle & no human intervention after installation]**
- **Operation in space, ISS, at 400km, no backgrounds from atmospheric interactions [extensive multi-step space qualification tests]**
- **Collection power: geometrical factor ($\approx 0.5 \text{ m}^2\text{sr}$) X exposure time (= ISS lifetime) [extensive calibration campaigns on ground]**

The AMS Project



AMS Collaboration

- 16 countries
- 60 institutes
- 500+ physicists
- 20 years

Project timeline

1994 CONCEPT



1998: STS-91



1997
AMS-01
PROTOTYPE



2000 @CERN
AMS-02 CONSTRUCTION



2008
@CERN
SC MAGNET
BEAM TEST



2010
TVT @ ESA (NL)

2010
@CERN
SC -> PM
NEW BEAM TEST



2011
@KSC
AMS-02
INTEGRATION & CR- μ RUN



MAY 2011
STS-134
FLIGHT



ON THE ISS

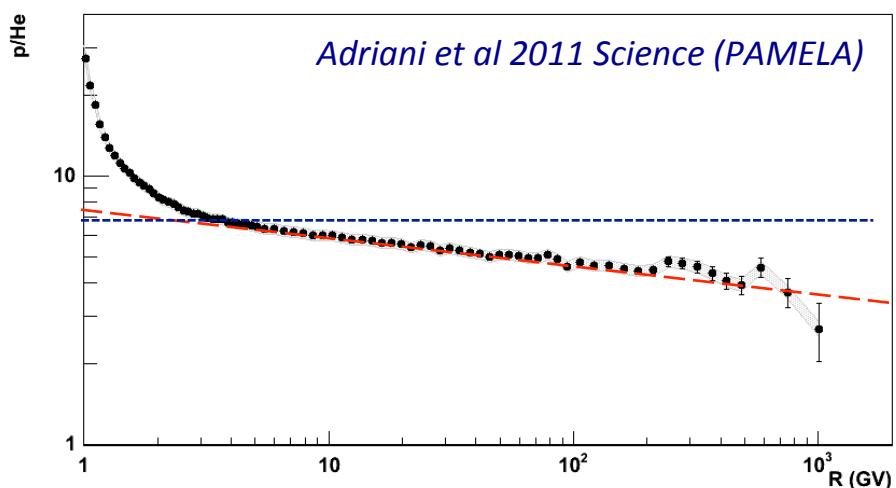


→ Steadily taking data on the ISS since May 19th 2011

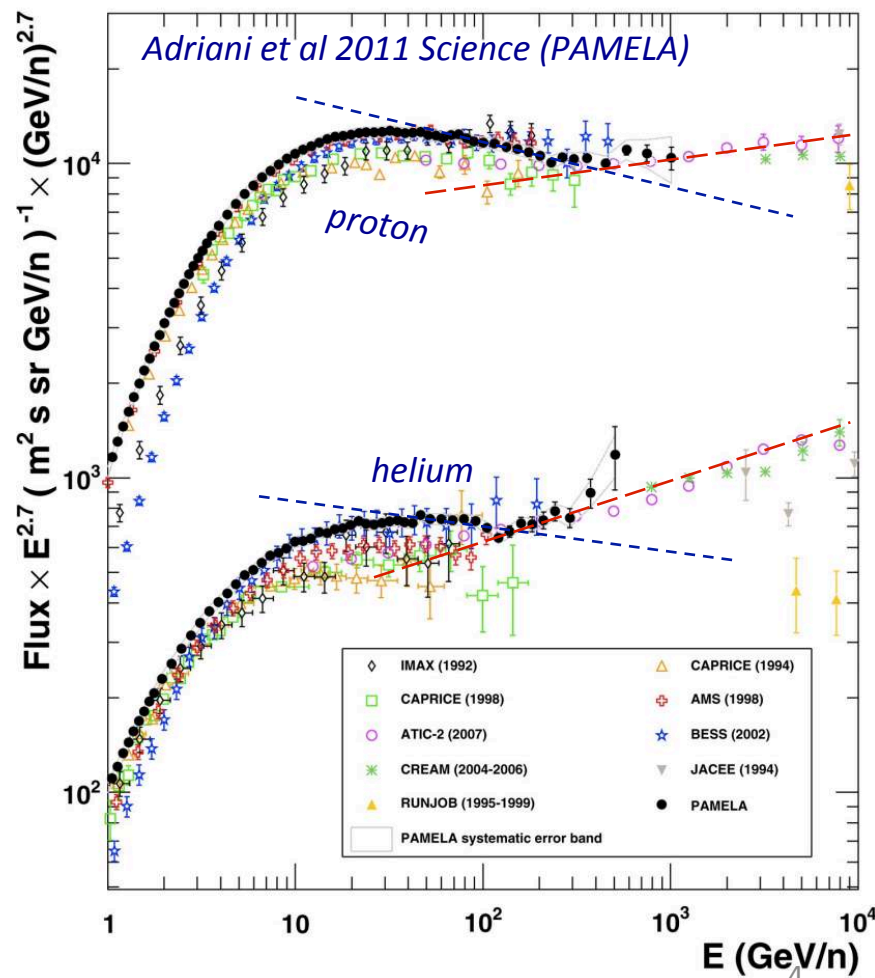
Cosmic-Ray Hadron Fluxes: a key science case

Proton and Helium spectra at high energies are revealing interesting spectral features that may offer a clue to the origin of the observed cosmic rays

- **High-energy Hardening:** multi-TeV energy spectra are harder than those at GeV-TeV
- **p/He anomaly:** Helium energy spectrum seems harder than that of the Hydrogen.
- **Sharp break?** Sharp transition located at 300 GV, as reported by PAMELA in 2011.



"These data challenge the current paradigm of cosmic-ray acceleration in supernova remnants followed by diffusive propagation in the Galaxy".



Spectral features in H and He

Basic predictions ($E \sim 10 \text{ GeV} - 100 \text{ TeV}$)

Based on many simplifying (and unjustified) assumptions:
homogeneity, isotropy, stationarity, linearity...

$$\left\{ \begin{array}{l} \text{DSA@SNRs: power-law } (\alpha \sim 2.0 - 2.2) \quad Q(E) \approx E^{-\nu} \\ \text{QLT: power-law diffusivity } (\delta \sim 0.3 - 0.6) \quad K(E) \approx E^{\delta} \\ \text{Equilibrium spectra } (E >> \text{GeV}) \quad \phi(E) \sim Q / K \approx E^{-(\nu+\delta)} \end{array} \right.$$

Deviations from power-law are unexplained by standard models of DSA acceleration and CR transport.

1) Intrinsic acceleration effects

- Non-linear DSA
- Mach number time-evolution

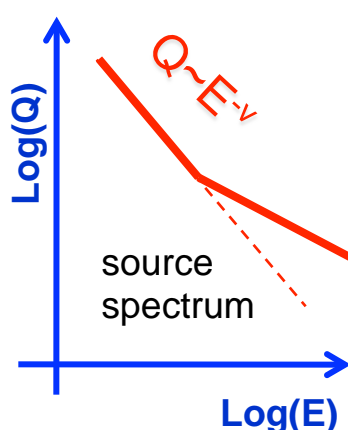
2) Propagation effects

- Transport in CR-induced turbulence
- Inhomogeneous diffusion coefficient

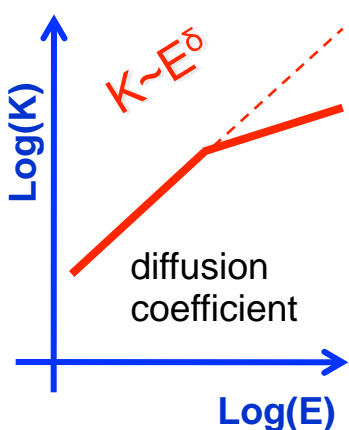
3) Multi-component nature of CR flux

- Local SNR + Galactic ensemble
- Reaccelerated CRs in weak shocks

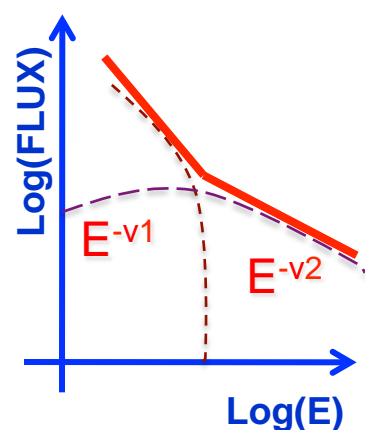
1) Acceleration, $Q(E)$



2) Propagation, $K(E)$



3) Multi-sources



p/He ratio: violation of universality in CR acceleration?

- Particle-dependent injection
- Non-uniform He distribution
- Non-DSA acceleration in
- Strong unaccounted spallation
-

Flux Measurement

Differential flux ($\text{m}^{-2} \text{sr}^{-1} \text{s}^{-1} \text{GV}^{-1}$)

$$\Phi(R) = \frac{N(R, R + \Delta R)}{\epsilon_{Trig}(R) \times A_{Tot}(R) \times T(R) \times \Delta R}$$

- R = p/Z, rigidity; important in magnetic spectrometers & CR astrophysics
N = Number of selected protons (helium) events in R,R+ΔR
T = Effective exposure time above geomagnetic cut-off (s)
 A_{Tot} = Total acceptance ($\text{m}^2 \text{sr}$) including geom factor + efficiencies
 ϵ_{Trig} = Trigger efficiency

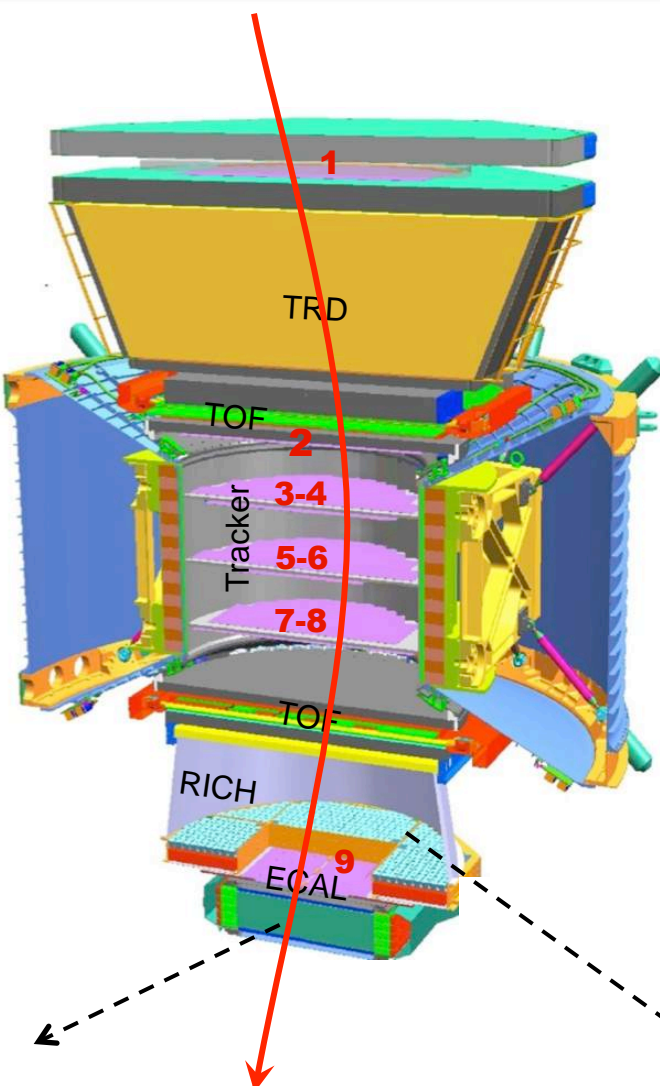
DATA/MC check

- Compute efficiencies
- Interaction studies

SPECTRAL UNFOLDING

- Resolution modeling
- Deconvolution algorithm

Multiple measurements of energy



Tracker, $R = p/Z$
 $MDR \approx 2TV (p); 3TV (He)$

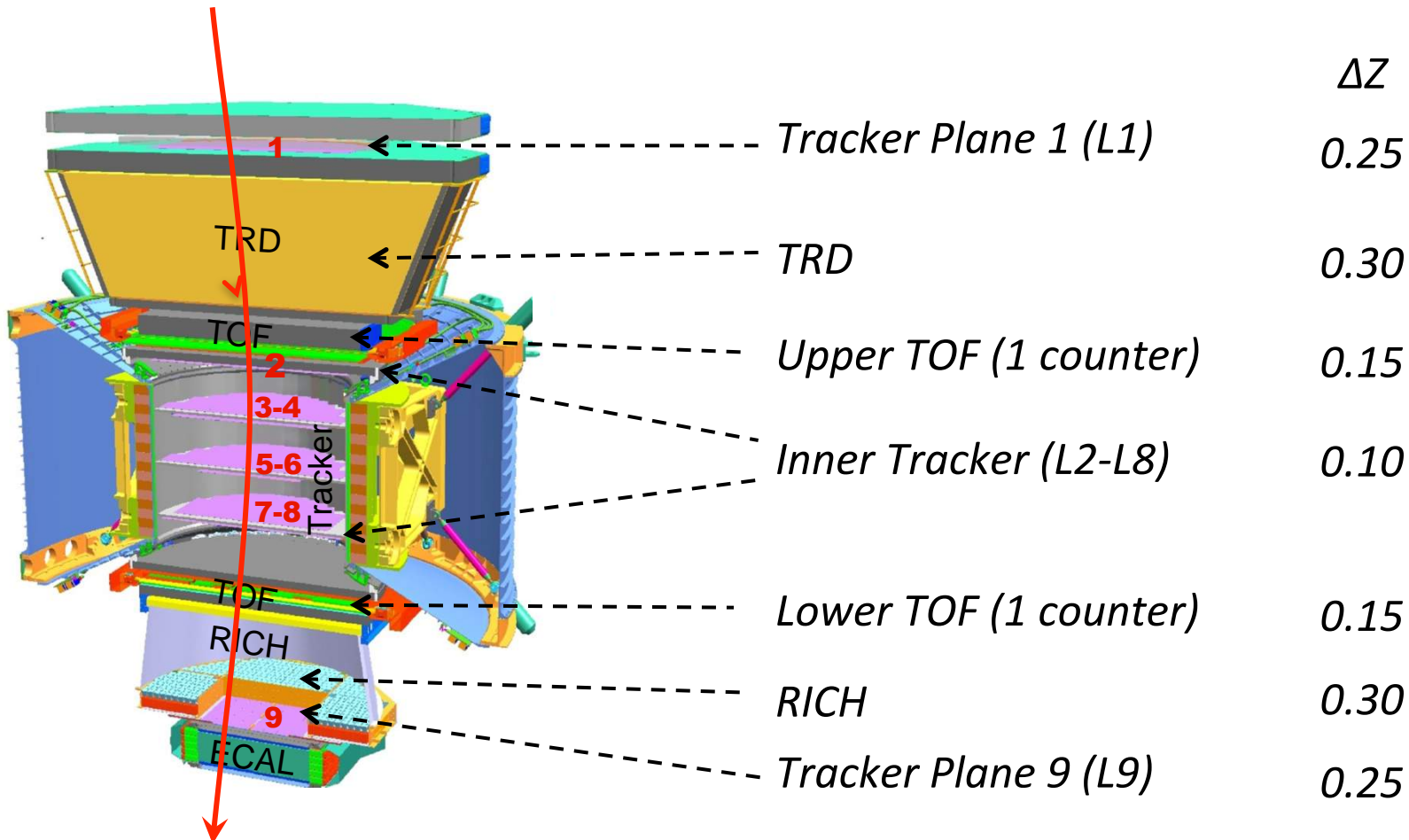
TOF, β
 $\Delta\beta/\beta \approx 1\%$

ECAL, E
 $\Delta E/E (\text{TeV } e^\pm) \sim 2\%$
 $\Delta E/E (\text{TeV } p) \sim 50\%$

RICH, β
 $\Delta\beta/\beta \approx 0.05\%$

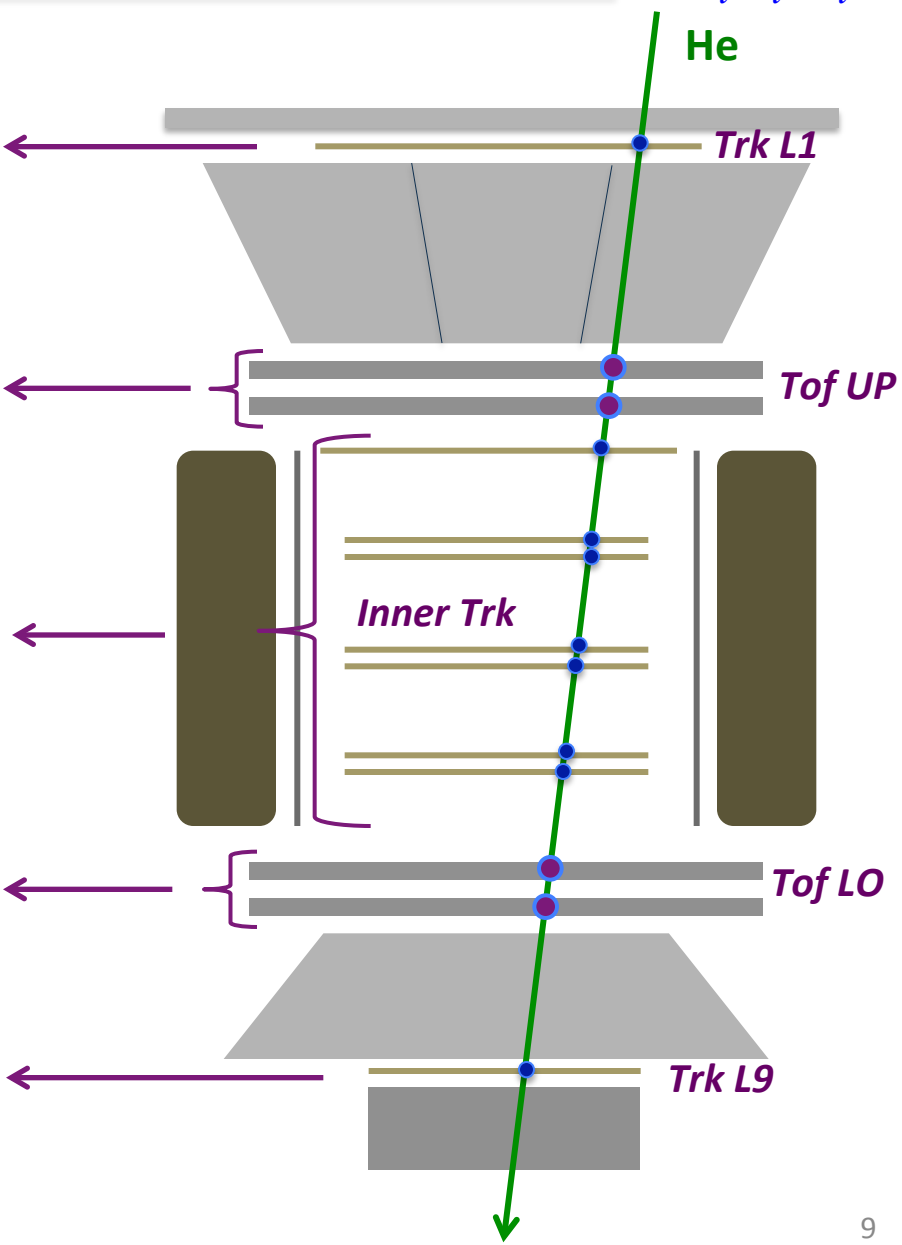
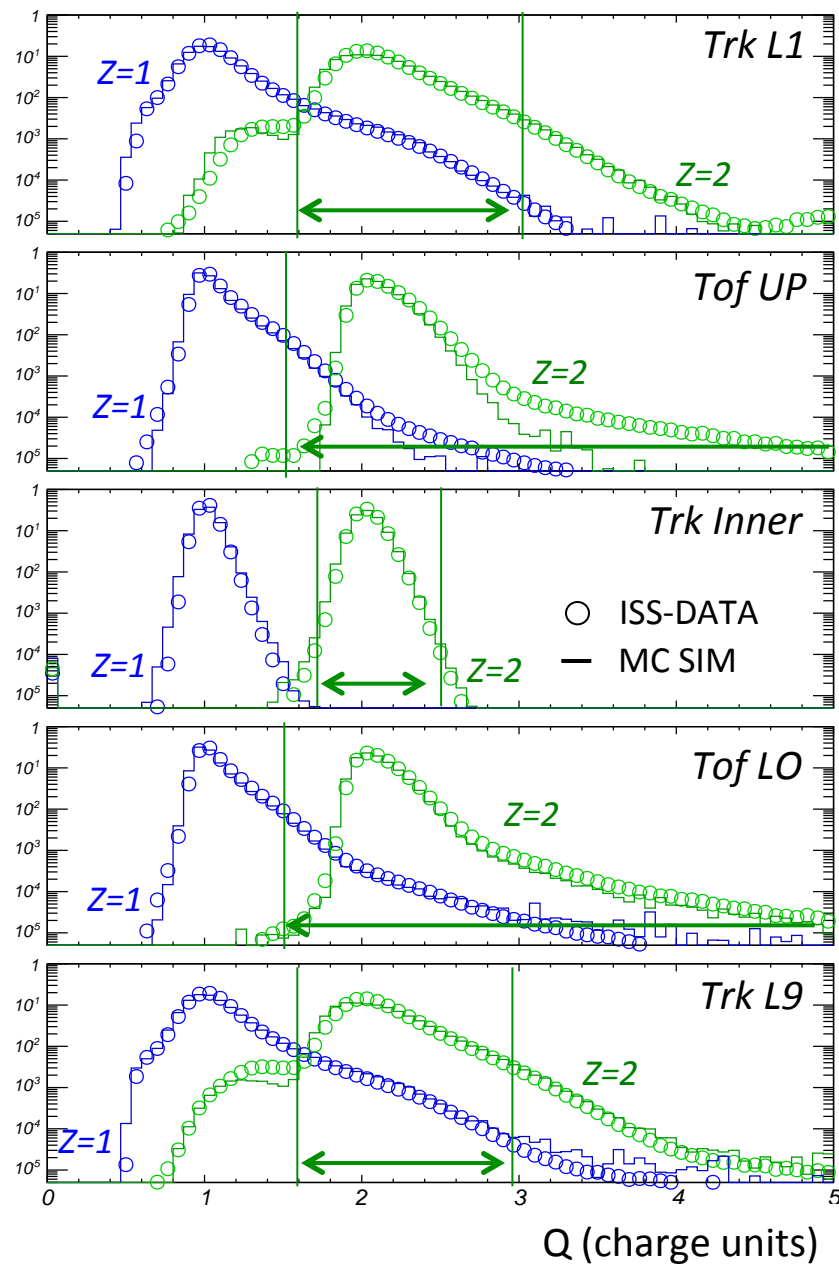
Geomagnetic cutoff, R
 $\Delta R/R \approx 10\% \text{ up to } \sim 25 \text{ GV}$

Multiple measurements of charge



Selection of Proton and Helium signals

$$\Phi_i(R_i) = \frac{N_i}{T_i \varepsilon_i A_i \Delta R_i}$$



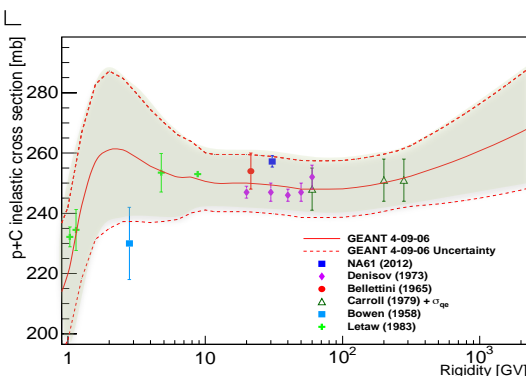
Acceptance

$$\Phi_i(R_i) = \frac{N_i}{T_i \varepsilon_i A_i \Delta R_i}$$

- ✓ Based on our MC simulation program.
- ✓ Detector response, signal digitization, and full analysis chain simulated.
- ✓ Data/MC corrections and several data-driven crosschecks performed.
- ✓ Role of interactions: flux attenuation in the detector material (C, Al)

Proton acceptance

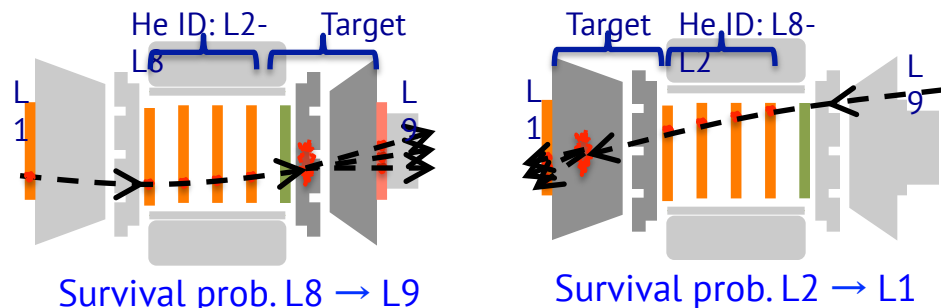
Cross-sections for proton interactions off detector material (C, Al) known to few percent at 1 GV and 1.8 TV.



~0.6 – 1 % systematic errors at GV – 2 TV

Helium acceptance

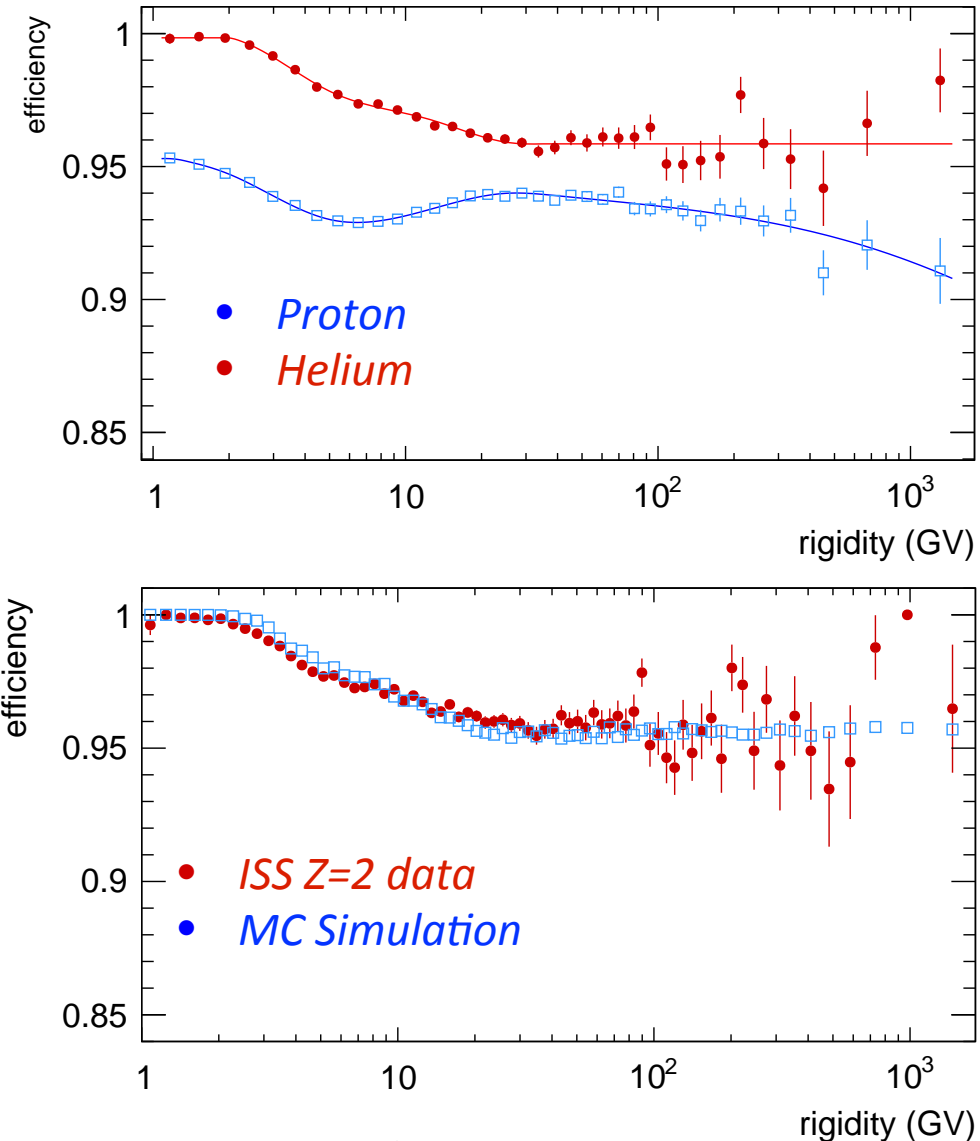
Helium collisions off C and Al: cross section data exist only below 10 GV
New method to determine interactions from ISS data with AMS pointing in horizontal direction



~1% < 200 GV increasing to ~2% at highest rigidities

Trigger Efficiency

$$\Phi_i(R_i) = \frac{N_i}{T_i \varepsilon_i A_i \Delta R_i}$$



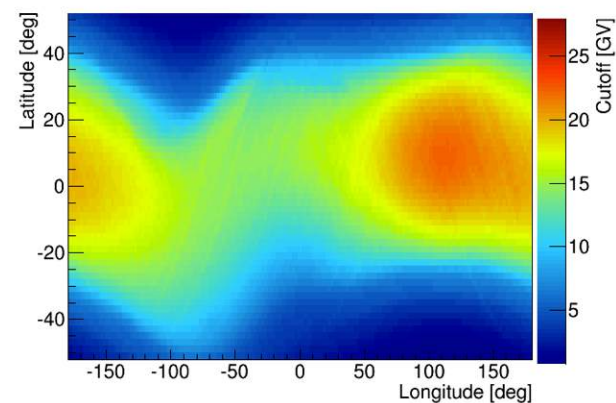
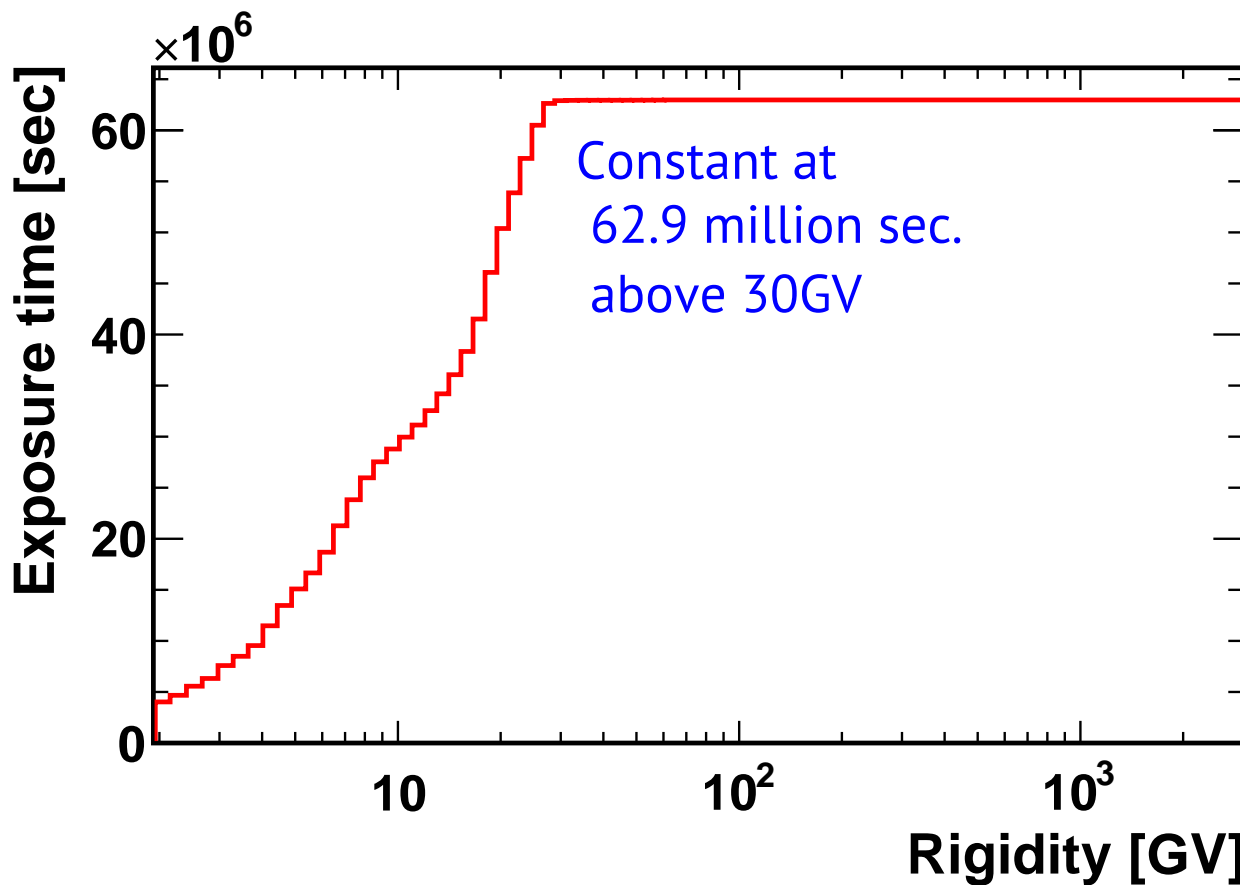
Trigger efficiency estimation can be done using flight data, thanks to a event sample collected with a dedicated minimum-bias trigger.

$$\varepsilon_{Trig} = \frac{N_{Phys}}{N_{Phys} + 100 \cdot N_{MinBias}}$$

Exposure Time

$$\Phi_i(R_i) = \frac{N_i}{T_i \varepsilon_i A_i \Delta R_i}$$

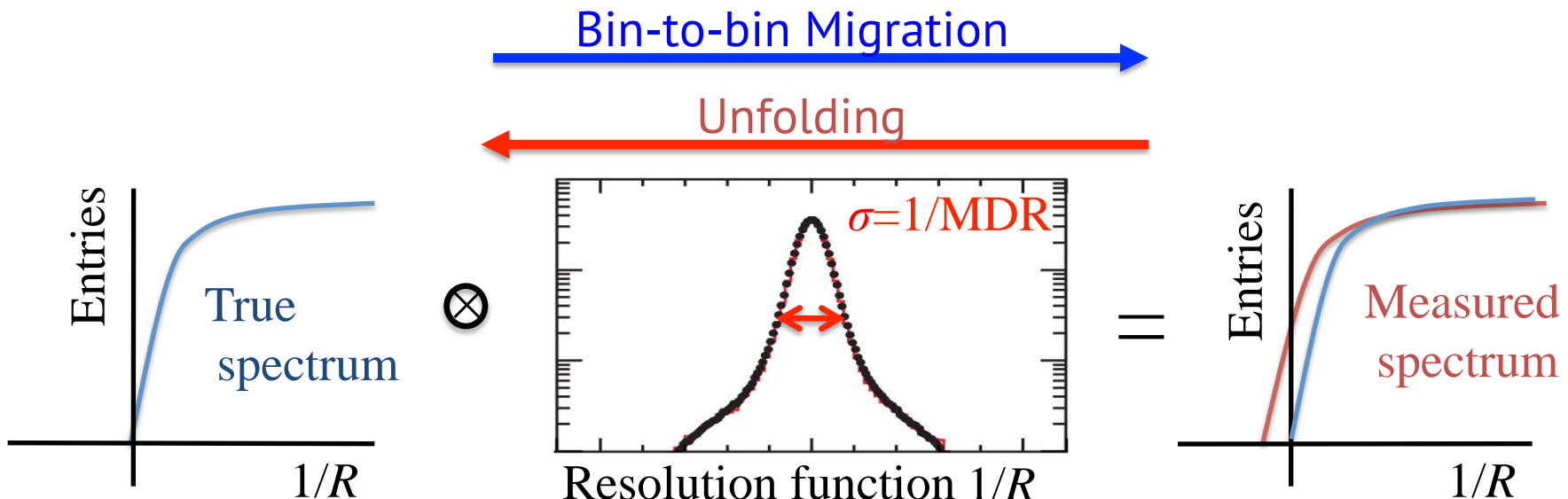
Exposure time “above cutoff” is function of rigidity
It depends on the ISS orbit along the geomagnetic field



Unfolding

Correction of bin-to-bin migration
is needed due to the finite
tracker resolution

$$\Phi_i(R_i) = \frac{N_i}{T_i \varepsilon_i A_i \Delta R_i}$$

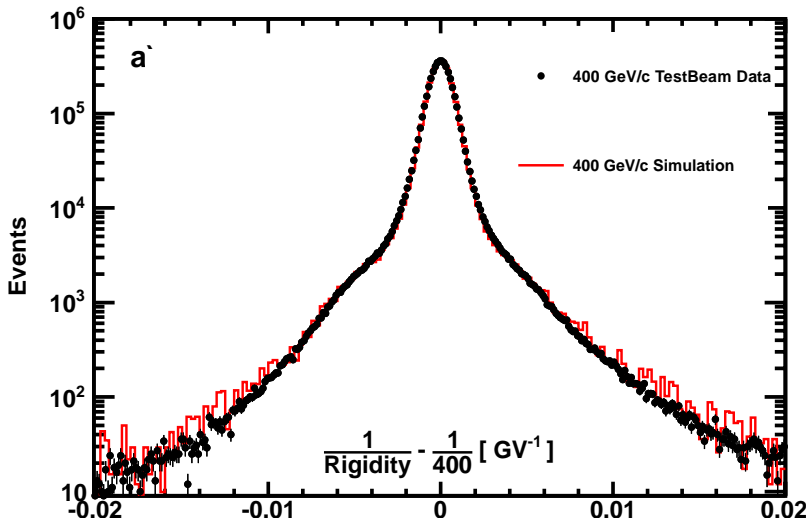


Difference between different unfolding algorithms gives a systematic error $\sim 0.5\%$

Tracker resolution

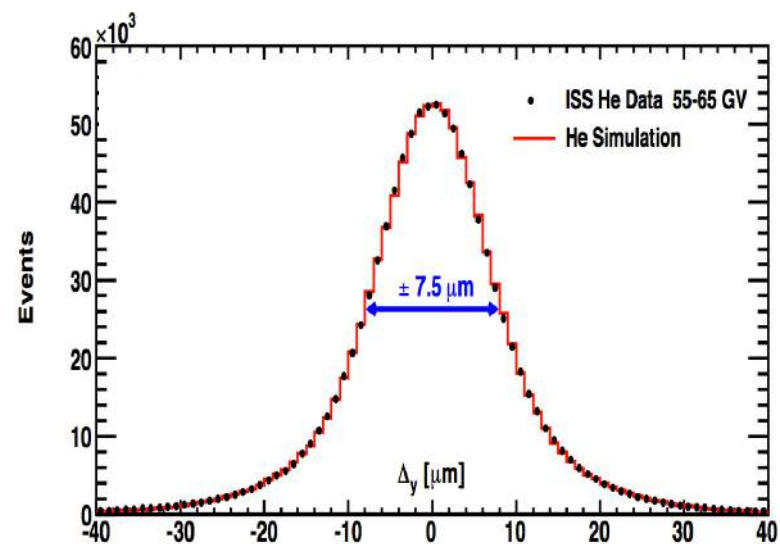
Protons:

- Resolution function from MC simulation
- Verified with:
 - 400 GeV/c Test Beams data
 - ISS data: tracker residuals, rigidity reconstruction (L1-L8) vs. (L2-L9)



Helium:

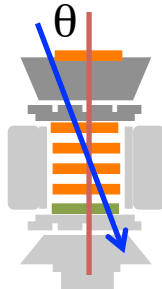
- Resolution function from MC simulation
- Verified with ISS data:
 - Tracker residuals
 - Rigidity reconstruction (L1-L8) vs. (L2-L9)



Uncertainty on the flux < 1% below 300 GV rising to 3% at 2 TV

Verifications: Protons

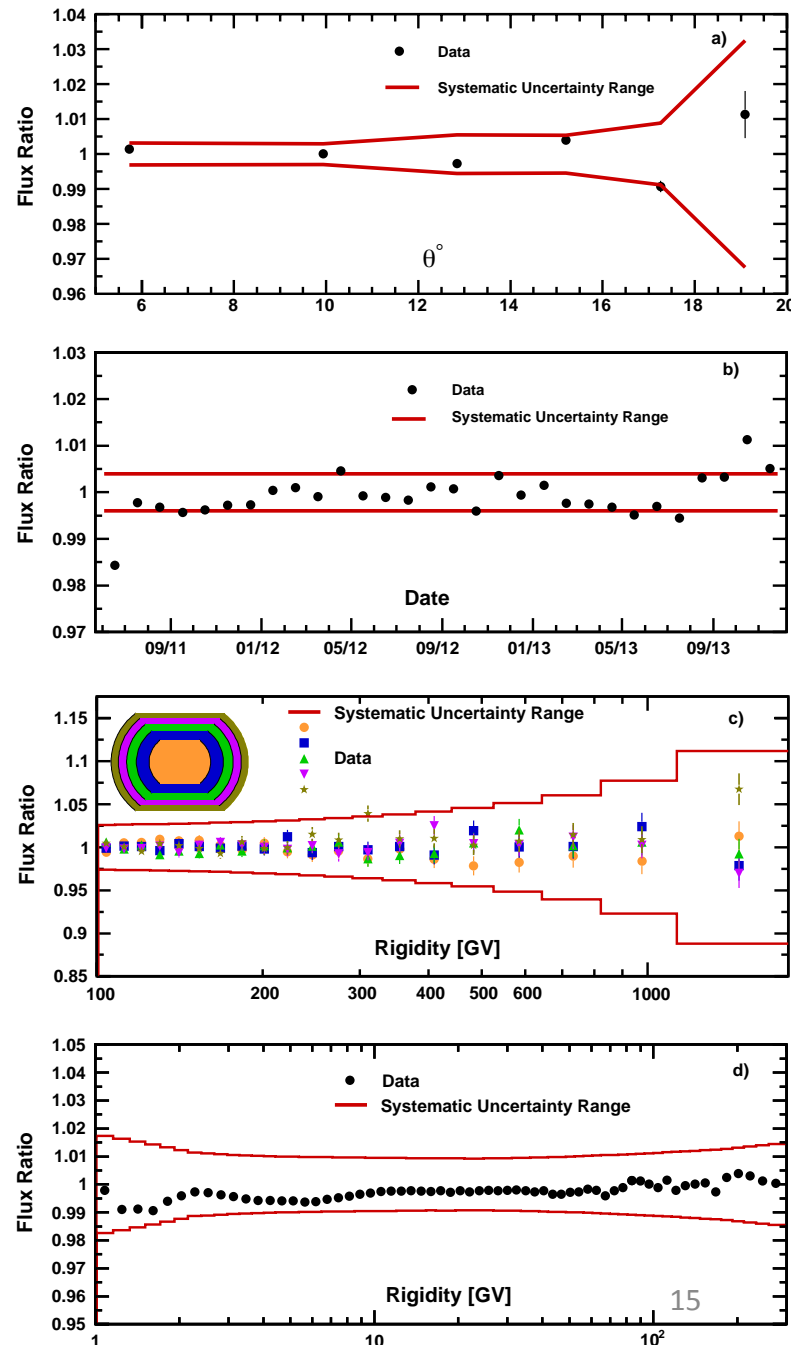
Angular dependence of measured flux at R>45 GV: to verify the systematic error assigned to the **acceptance**.



Time dependence of the high-energy flux: at R>45 GV no observable effects from solar modulation. This verifies that the **detector performance is stable**.

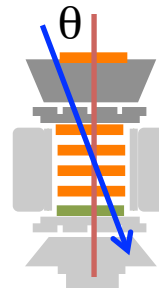
Flux reconstruction in different TOI entry regions of the acceptance. Verification of errors assigned to the tracker alignment.

Measured flux using **inner tracker**, i.e., with a different resolution and MDR. This verifies the errors on **rigidity resolution function and unfolding procedure**



Verifications: Helium

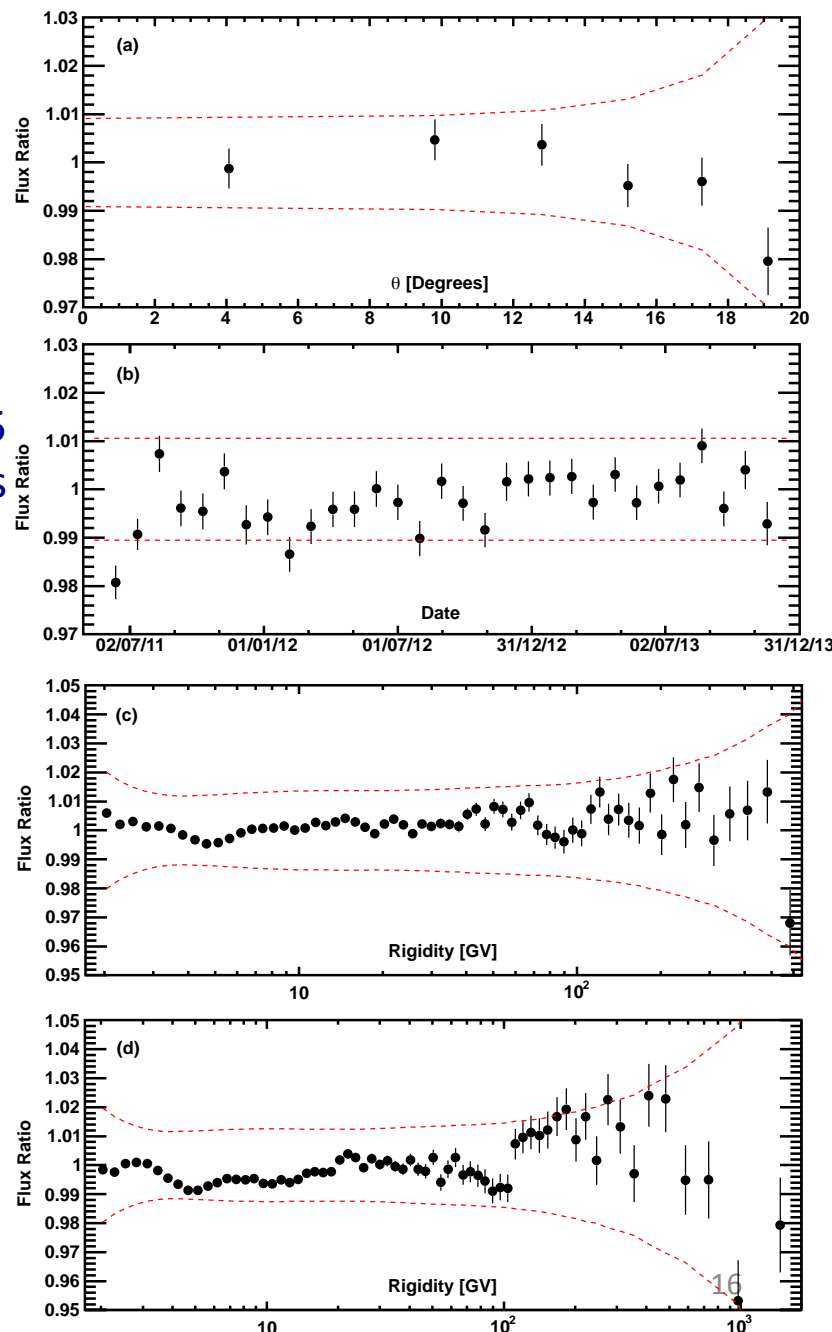
Angular dependence of measured flux at R>45 GV: to verify the systematic error assigned to the **acceptance**.



Time dependence of the high-energy flux: at R>45 GV no observable effects from solar modulation. This verifies that the **detector performance is stable**.

Measured flux using different tracker patterns (**inner-tracker+L1**) with a different resolution and MDR. This verifies the errors on **rigidity resolution function and unfolding procedure**

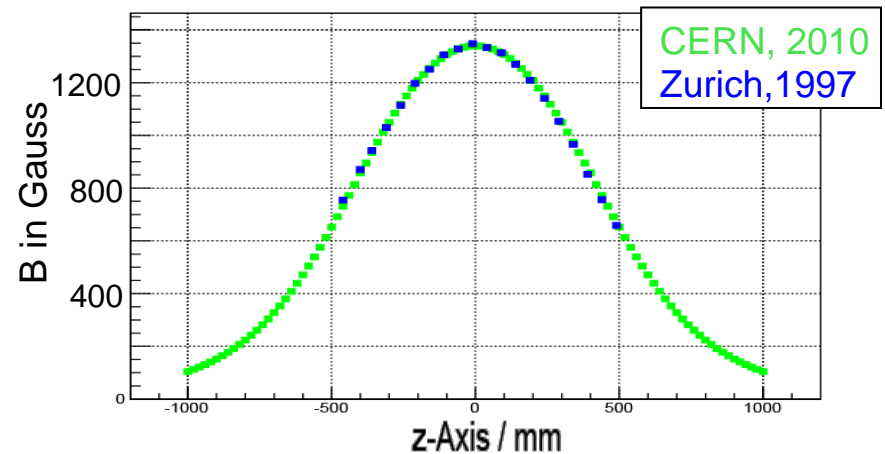
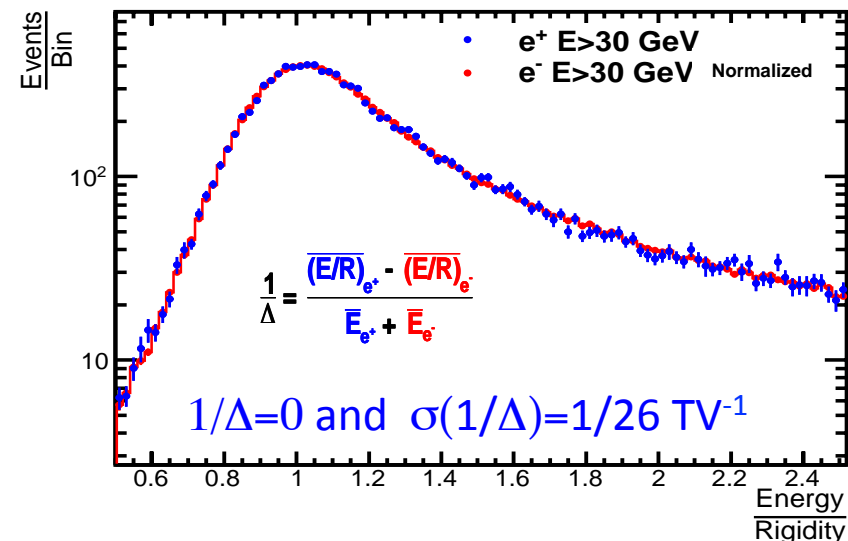
Measured flux using **inner tracker**, i.e., with a tracker pattern of different rigidity resolution and MDR. This verifies the errors on **rigidity resolution function and unfolding procedure**



Absolute Rigidity Scale

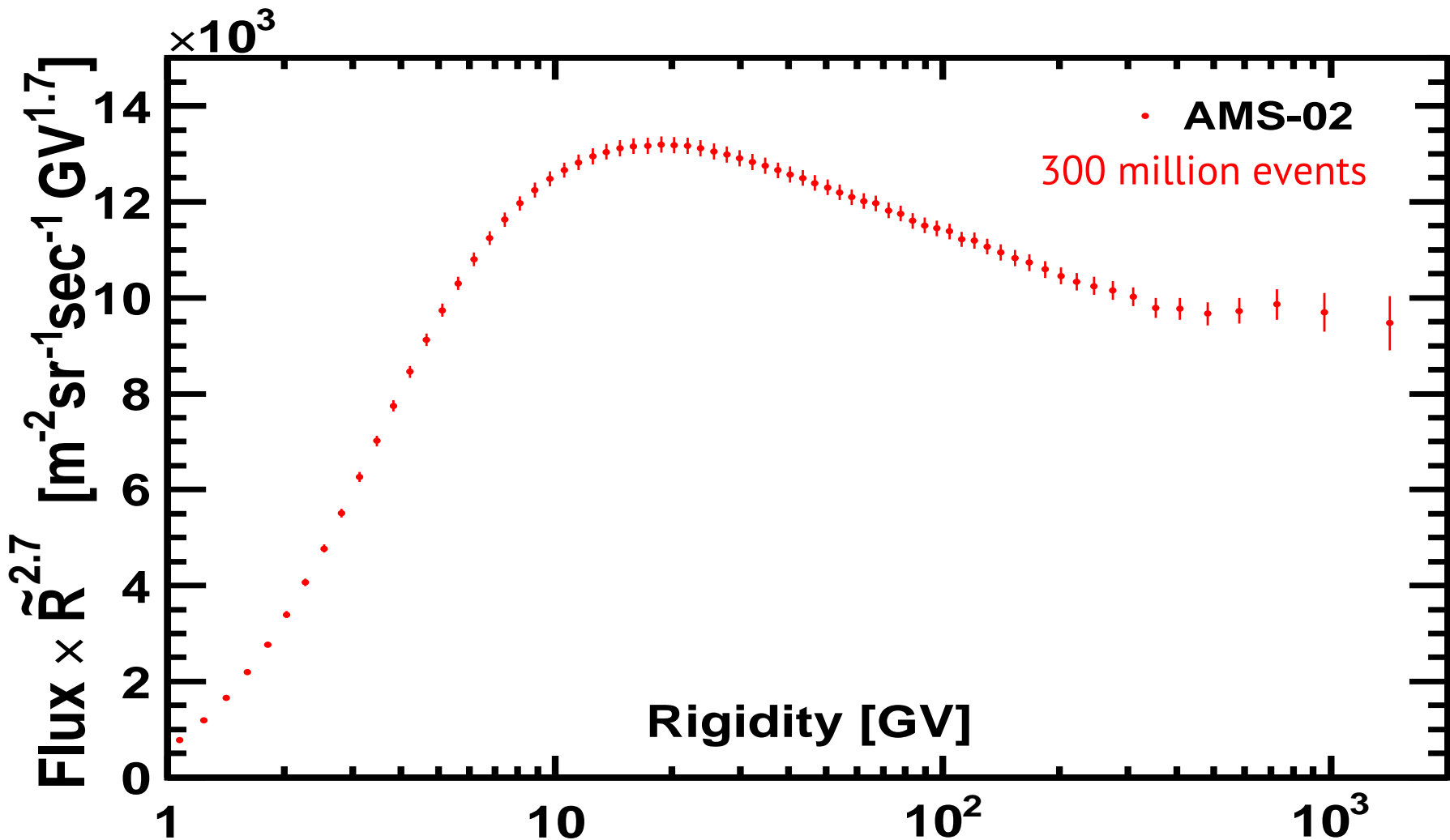
Two contributions to the uncertainty:

1. **Residual tracker misalignment ($1/\Delta$):**
checked with $E_{ECAL}/R_{Tracker}$ ratio for **electrons and positrons**, limited by the current high energy positron statistics.
Corresponding flux error: 2.5% @1 TV.
2. **Magnetic field:**
Mapping measurement (0.25%) and temperature corrections (0.1%).
Flux error: less than 0.5% at all rigidity

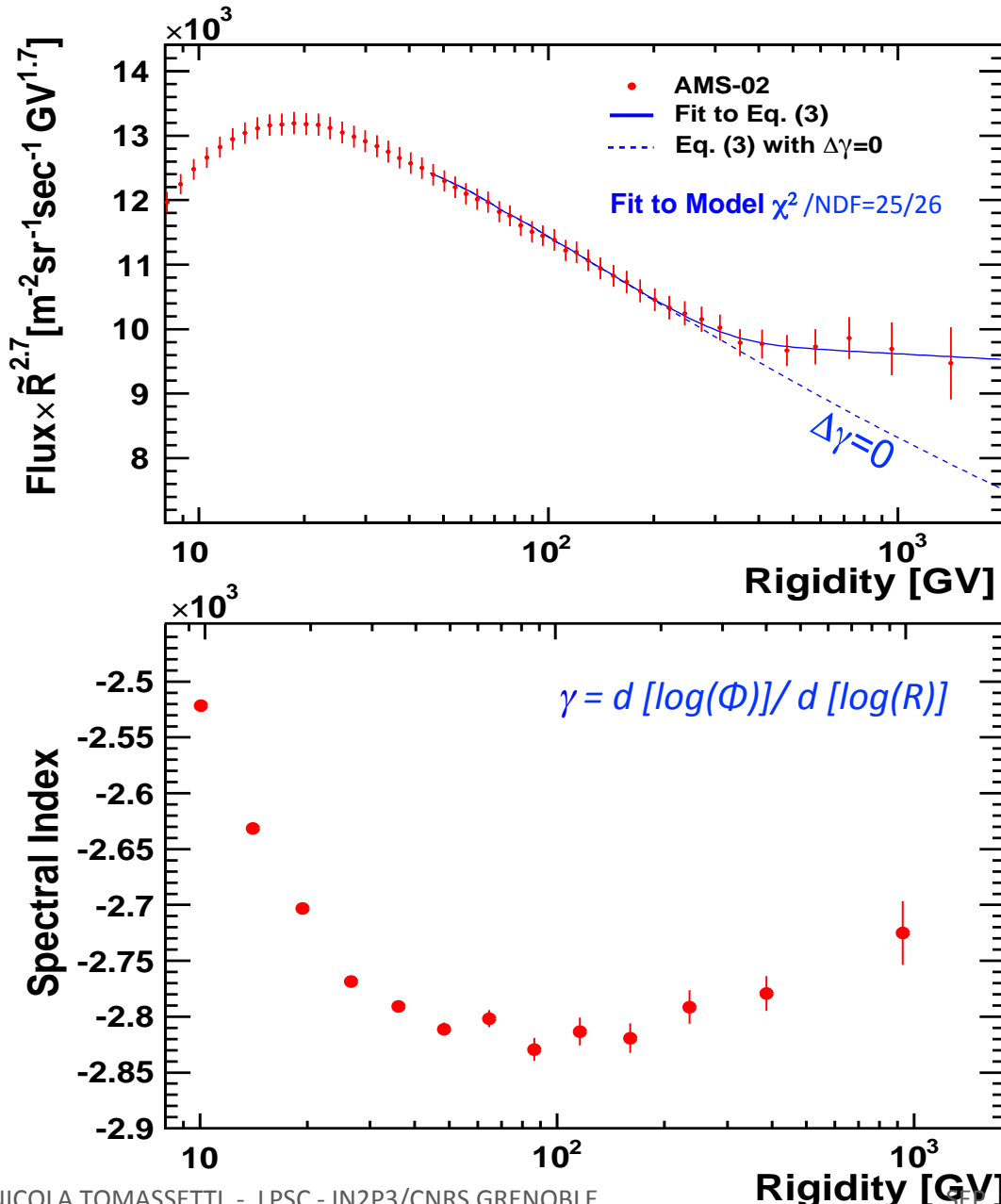


Proton Flux

Phys. Rev. Lett. 114, 171103



Proton Flux



The spectrum cannot be described by a single power-law function. We obtain a good description using a double power-law:

$$\Phi = C \left(\frac{R}{45 \text{ GV}} \right)^\gamma \left[1 + \left(\frac{R}{R_0} \right)^{\Delta\gamma/s} \right]^s$$

$\gamma = -2.849^{+0.002}_{-0.002}(\text{fit})^{+0.004}_{-0.003}(\text{sys})$ low-rigidity slope

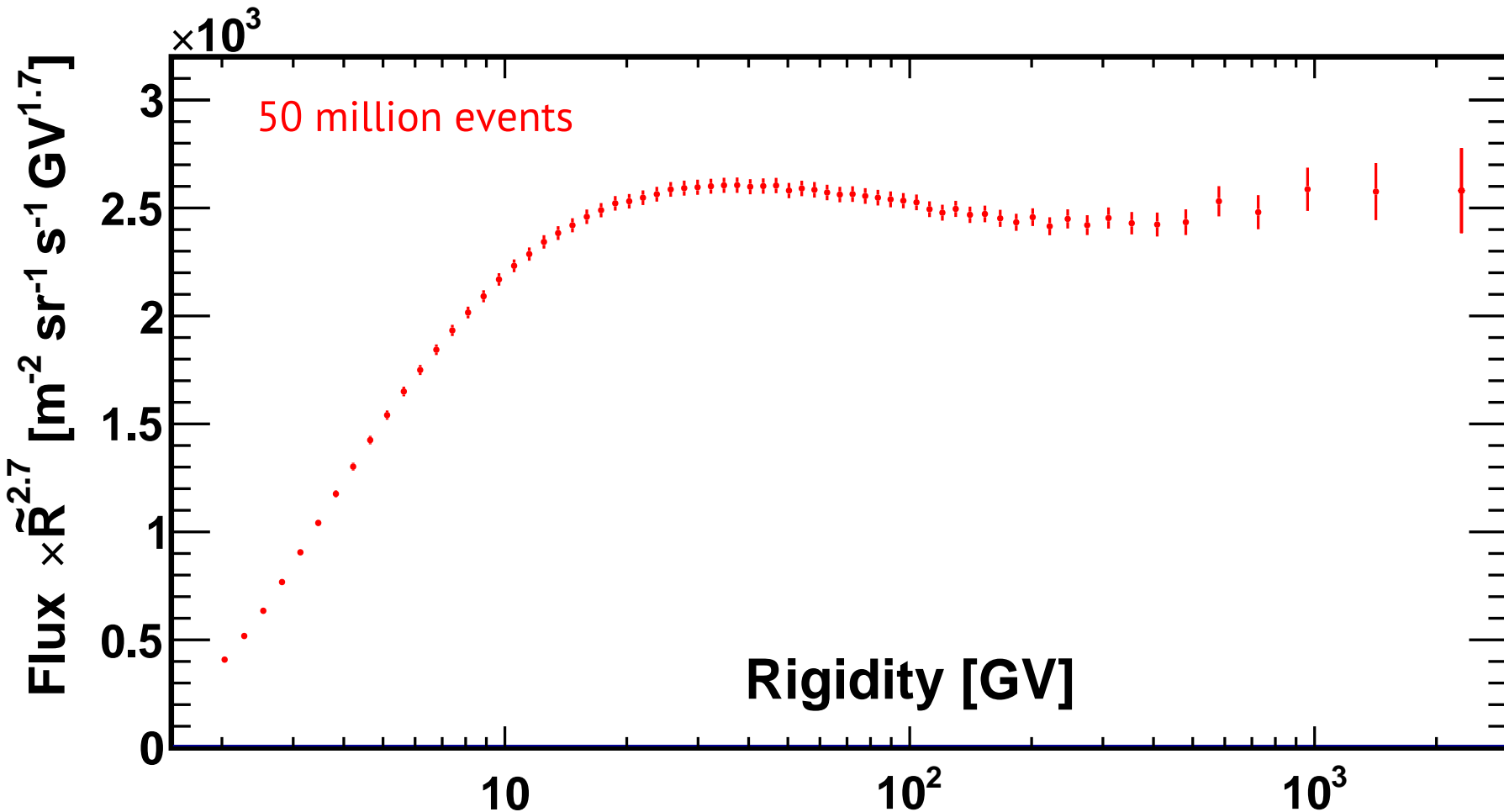
$\Delta\gamma = 0.133^{+0.032}_{-0.021}(\text{fit})^{+0.046}_{-0.030}(\text{sys})$ delta-slope

$R_0 = 336^{+68}_{-44}(\text{fit})^{+66}_{-28}(\text{sys}) \text{ [GV]}$ critical rigidity

The detailed variation of the high-energy flux can be characterized by measuring the log-slope. As shown, the proton flux experiences a progressive hardening above ~ 100 GV of rigidity.

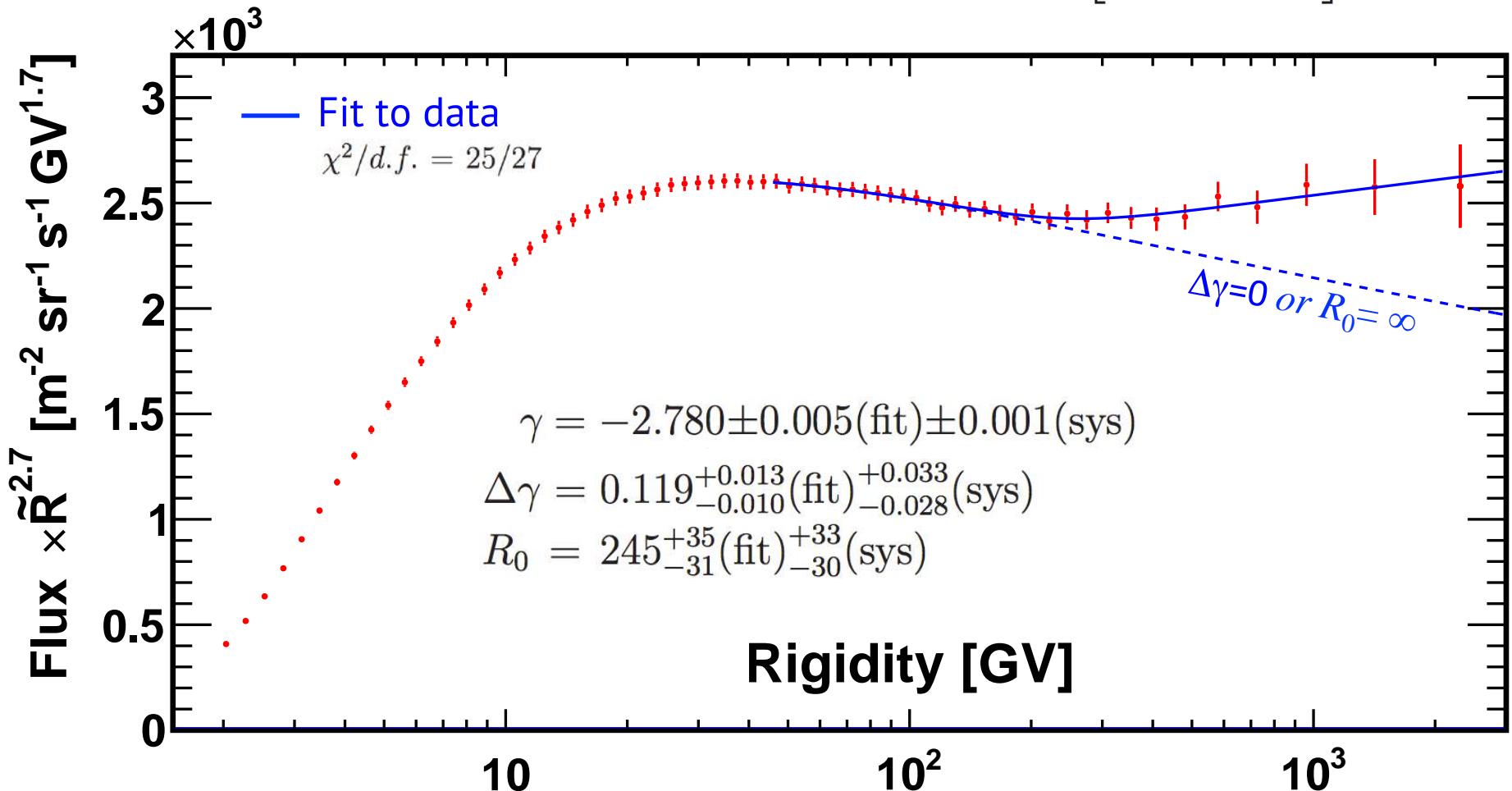
Helium Flux

to appear in PRL - November 2016 issue – Editors' suggestion

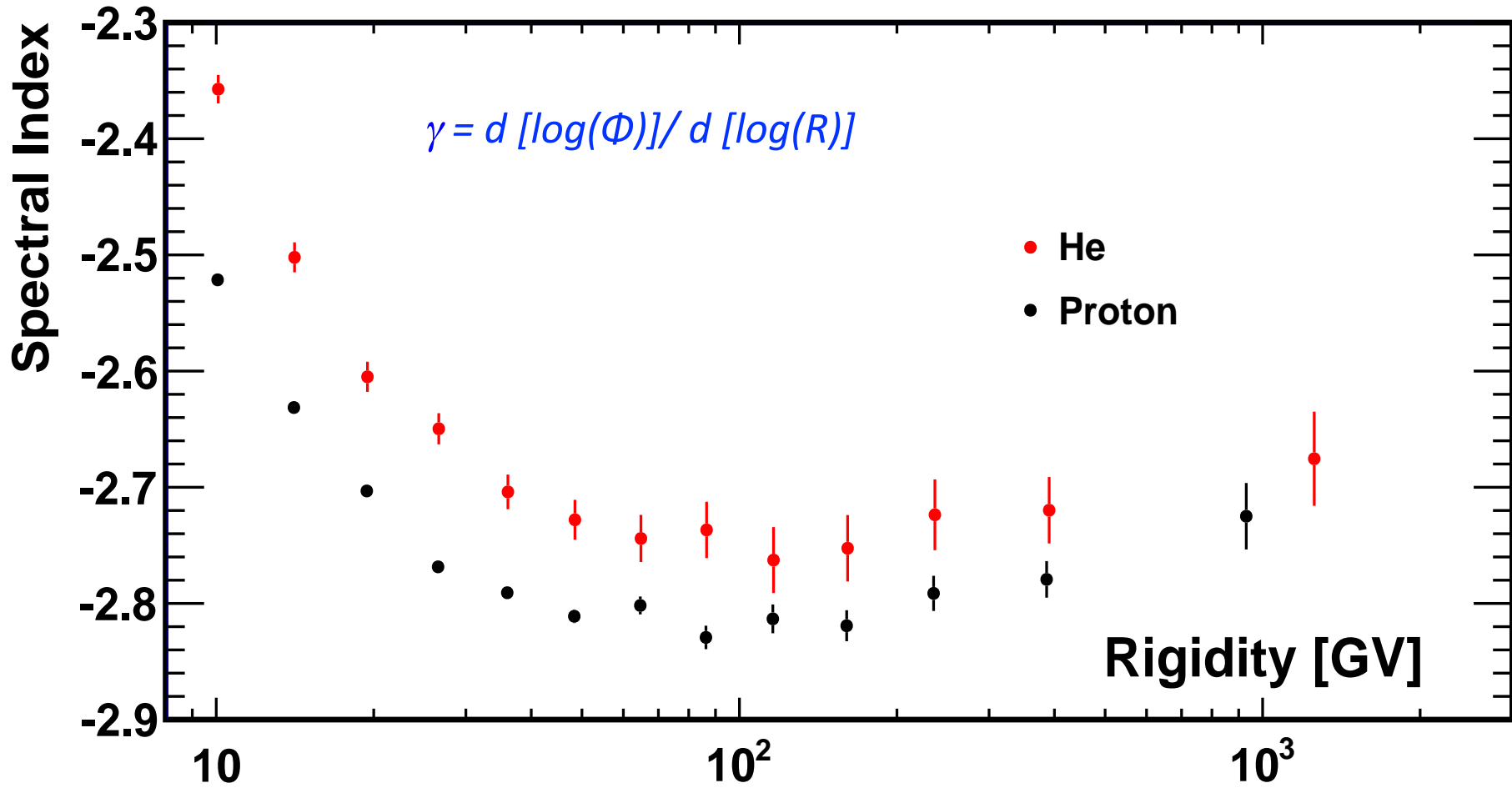


Helium Flux

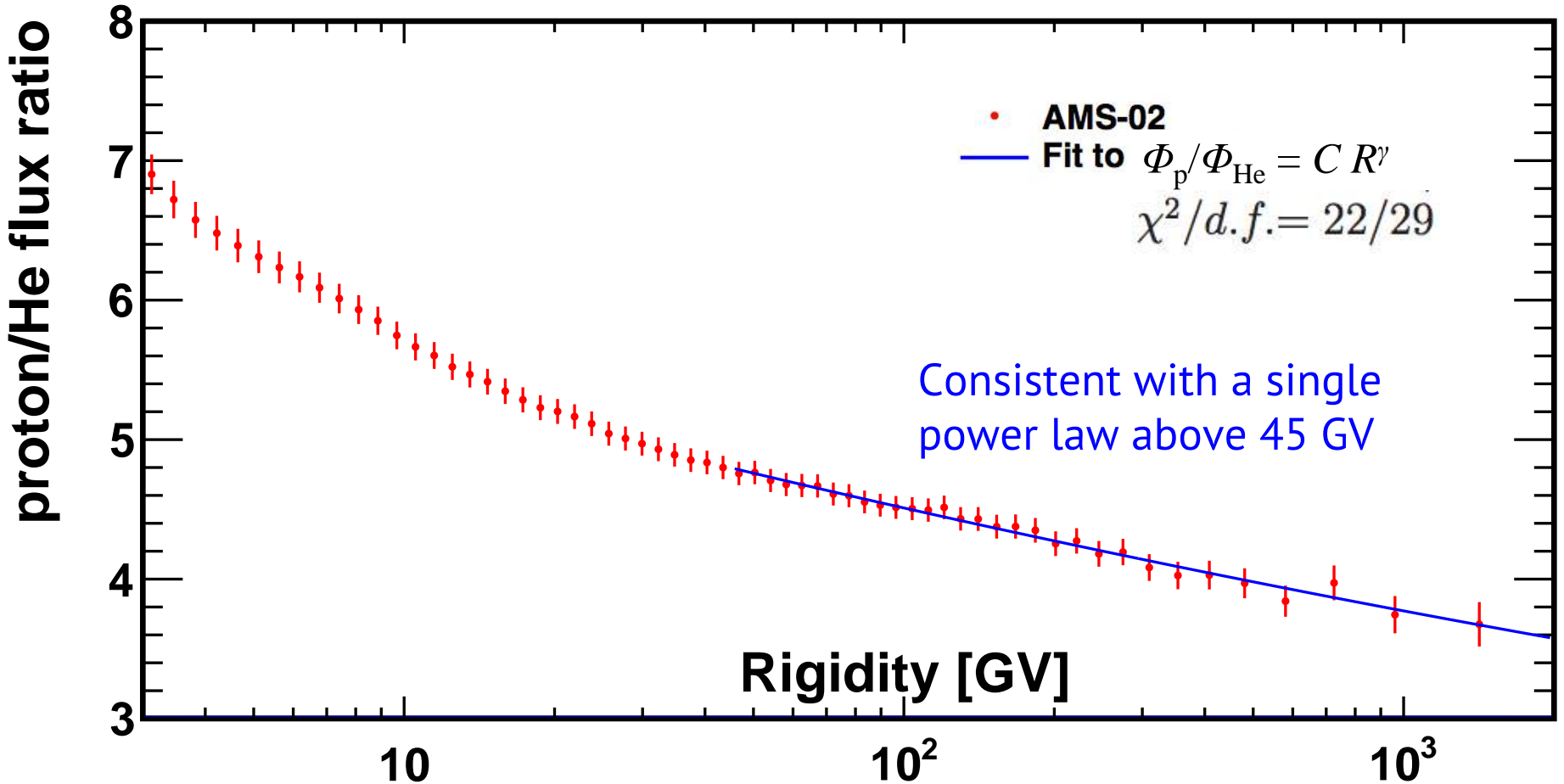
Double Power Law: $\Phi = C \left(\frac{R}{45 \text{ GV}} \right)^\gamma \left[1 + \left(\frac{R}{R_0} \right)^{\Delta\gamma/s} \right]^s$



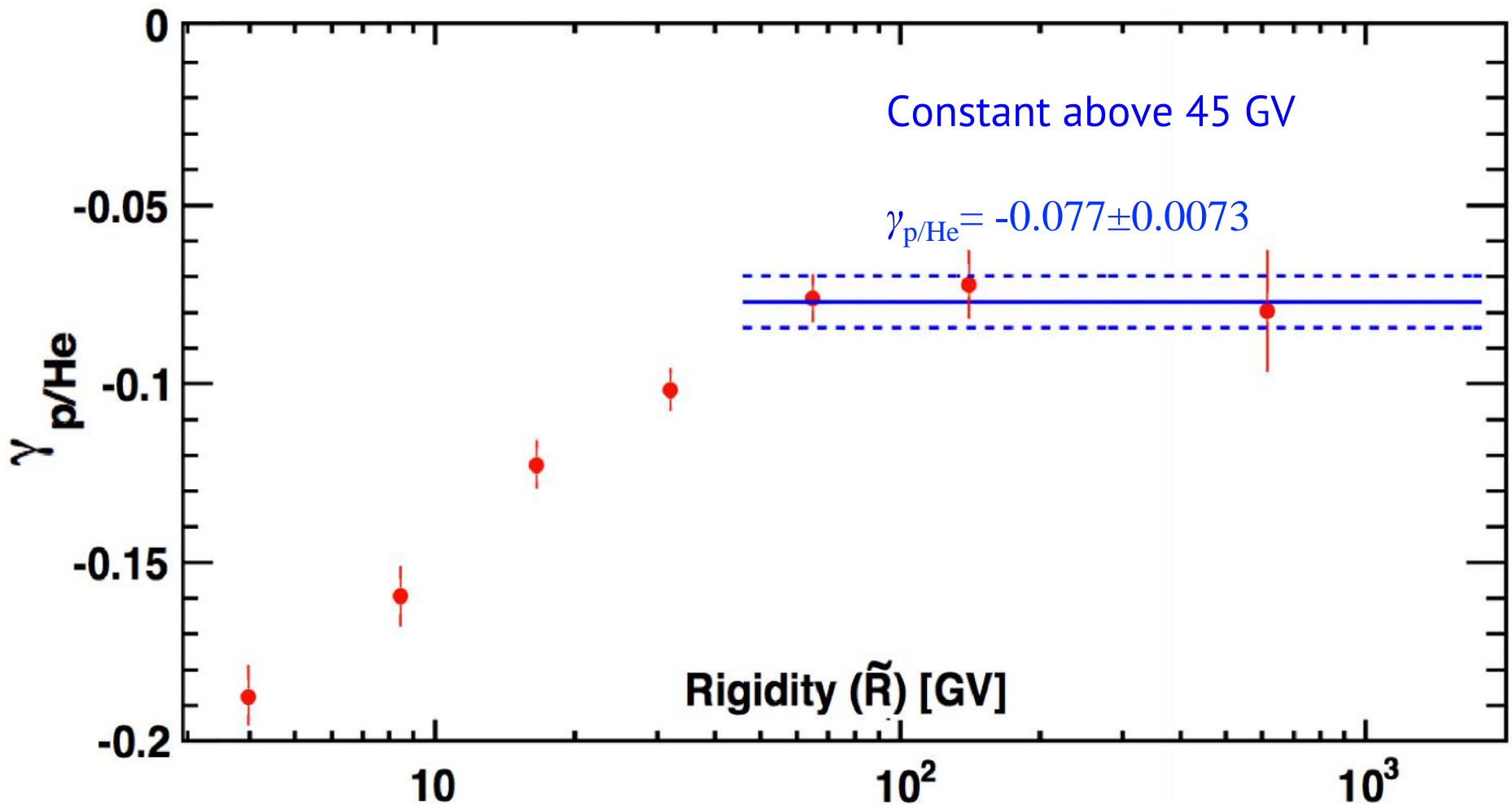
Helium Spectral Index



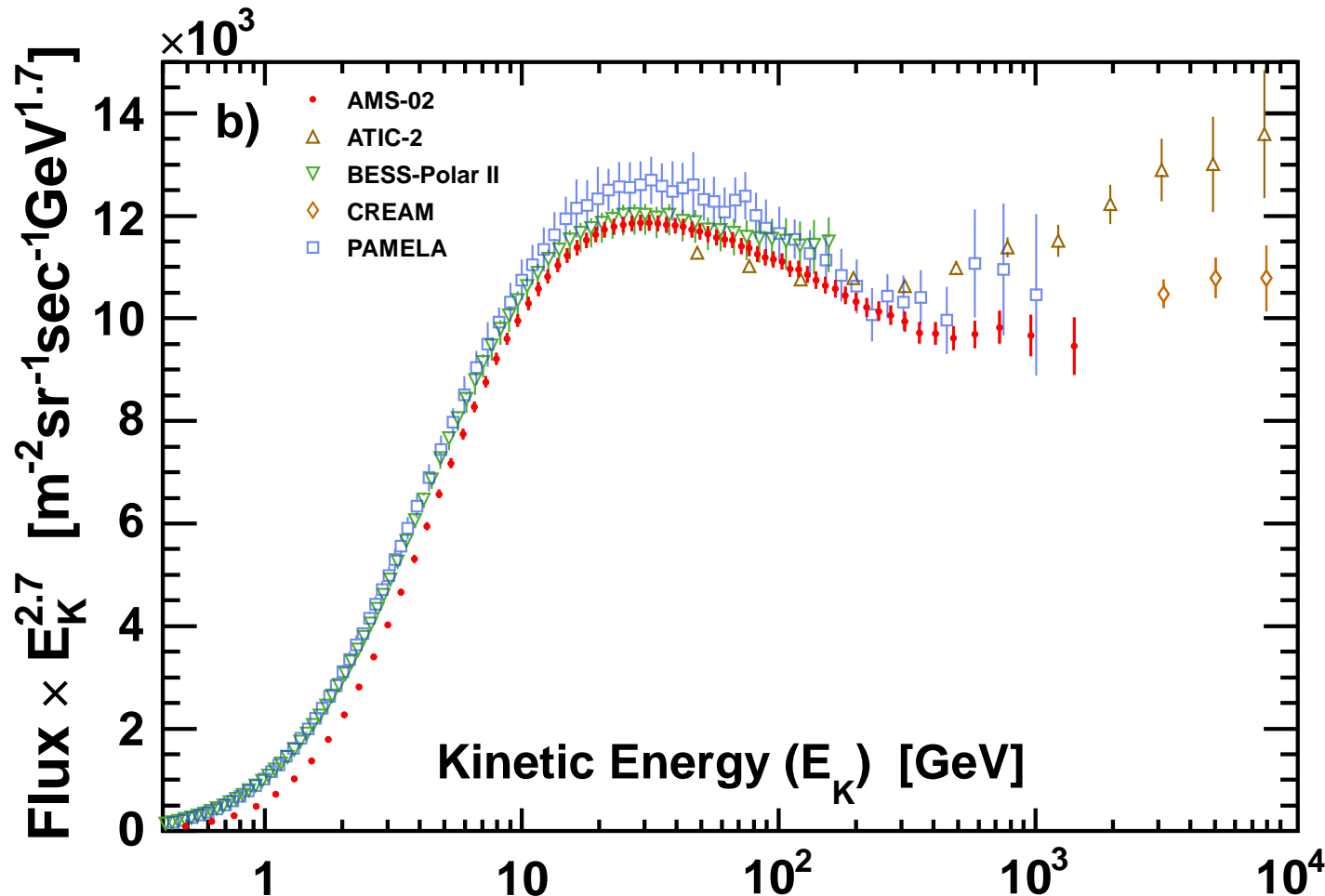
Proton/Helium Flux Ratio



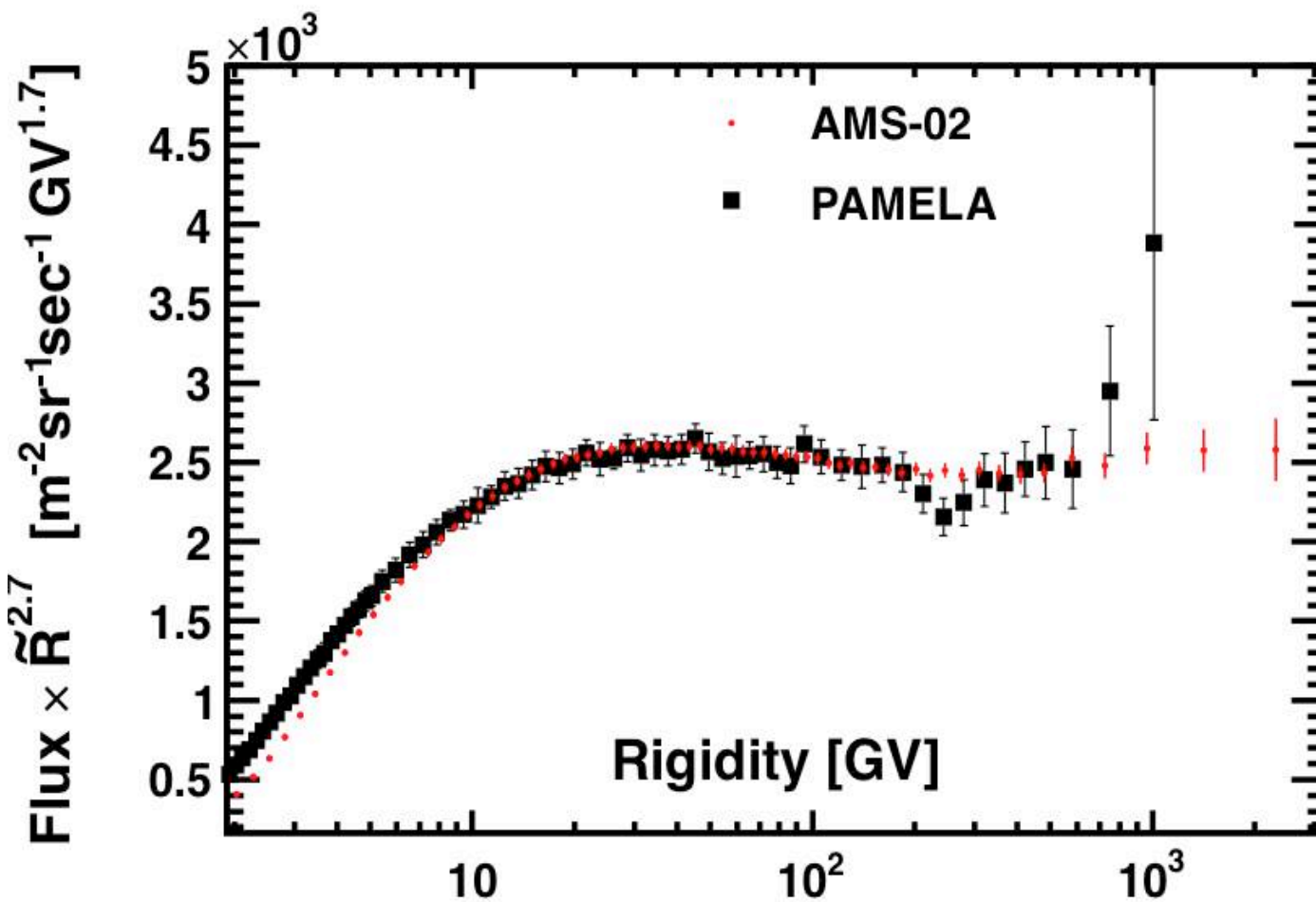
Proton/Helium Ratio Spectral Index



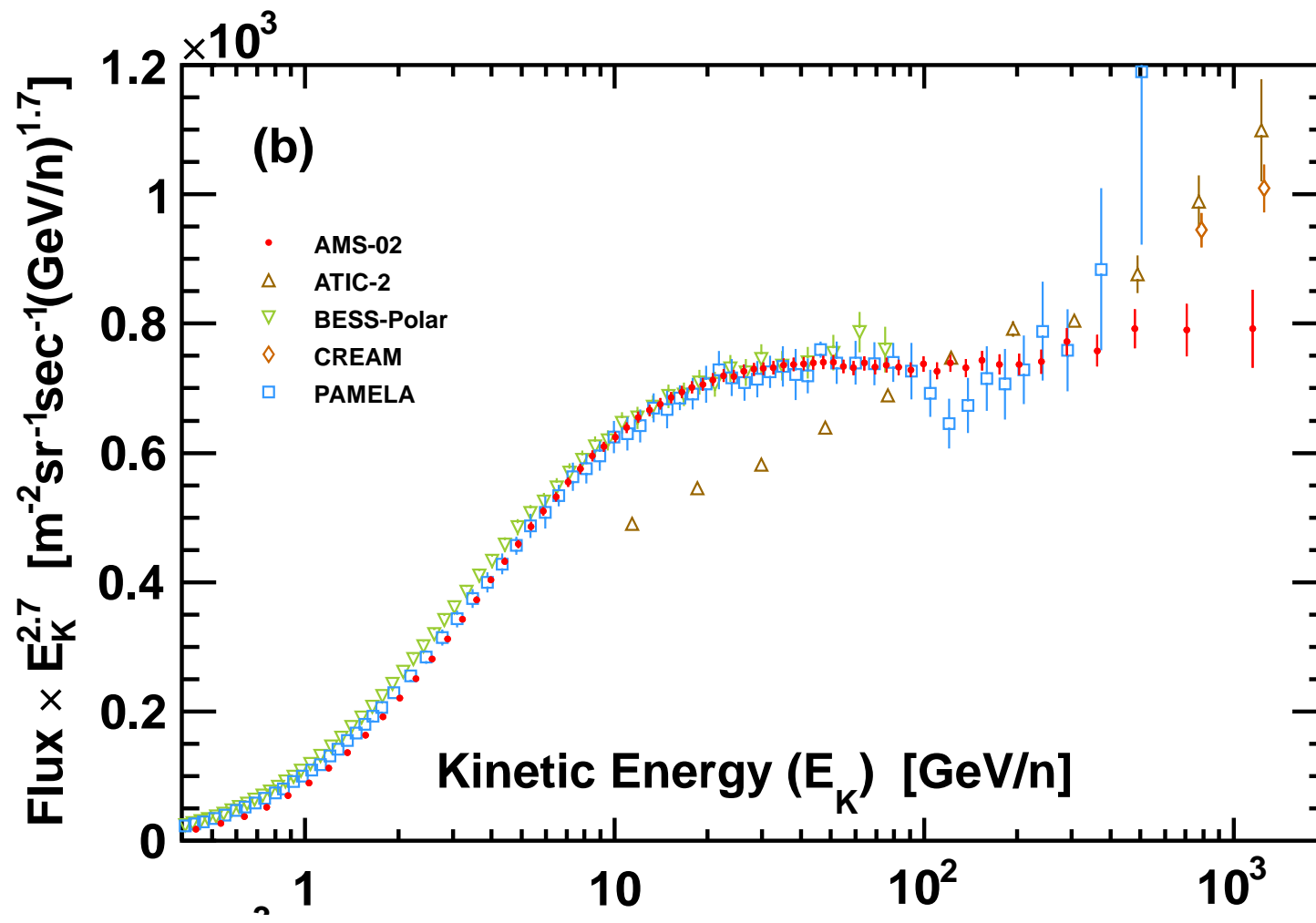
Proton Flux VS Kinetic energy



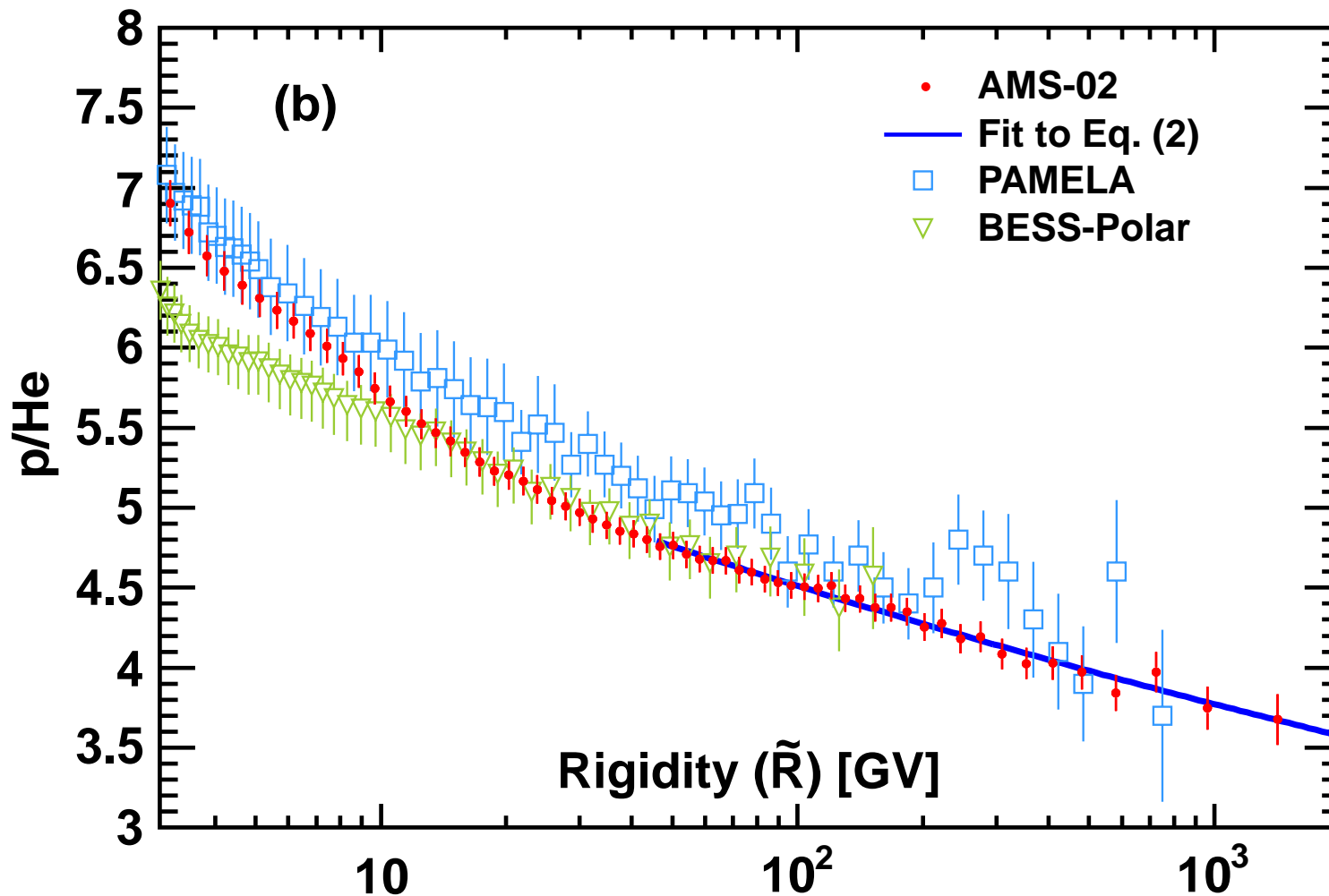
Helium Flux VS rigidity



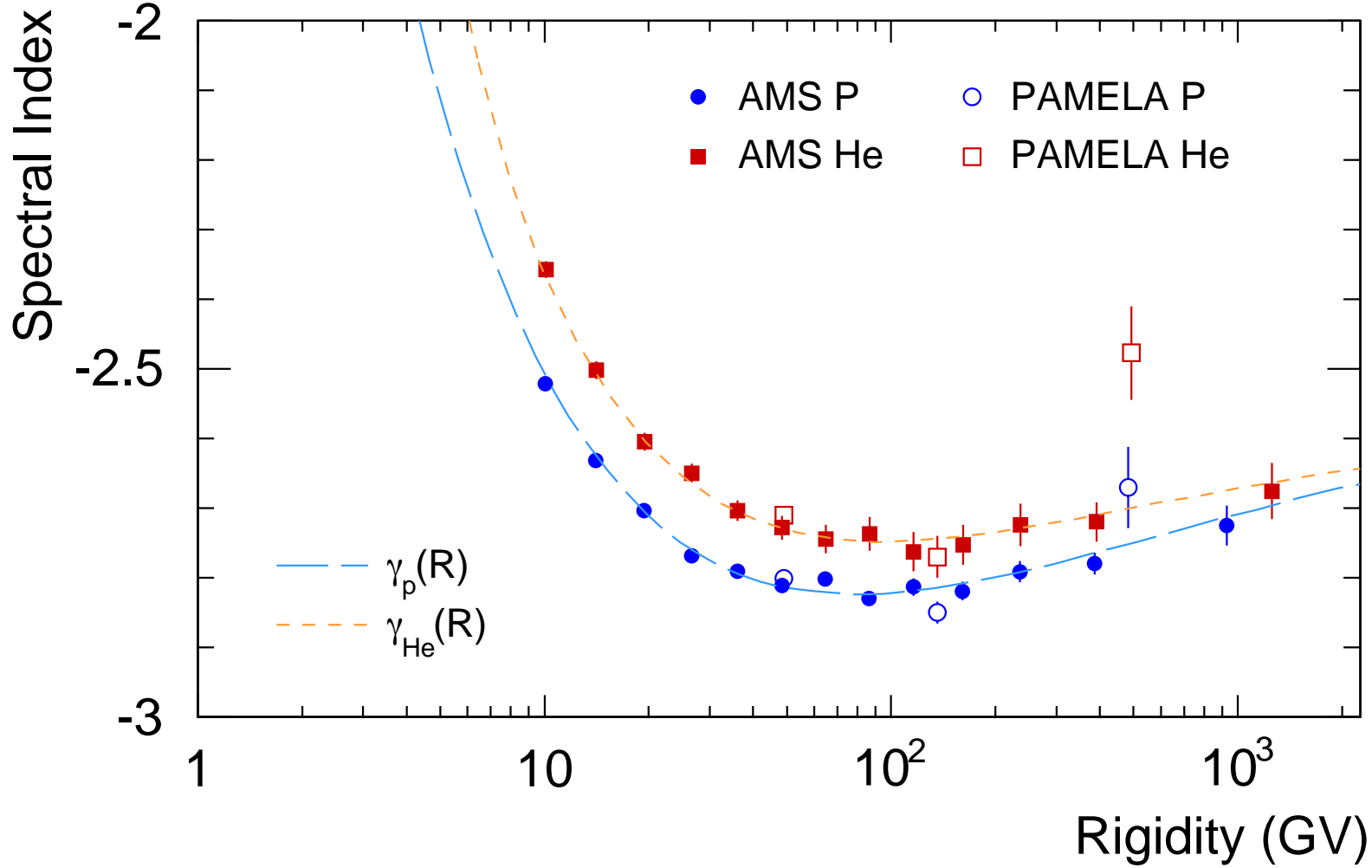
Helium Flux VS Kinetic energy per nucleon



p/He ratio as function of rigidity



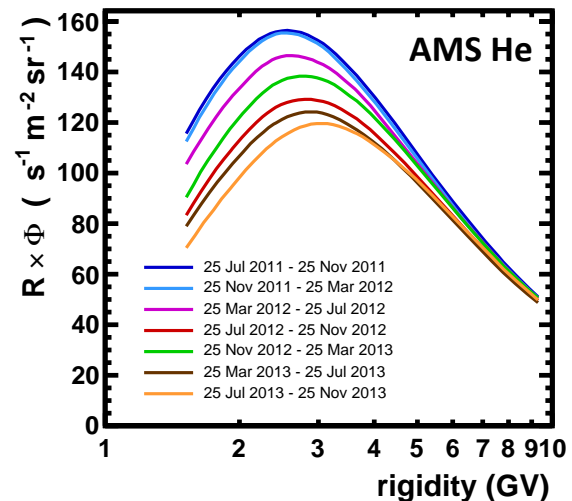
Proton & He Spectral Index



Conclusions

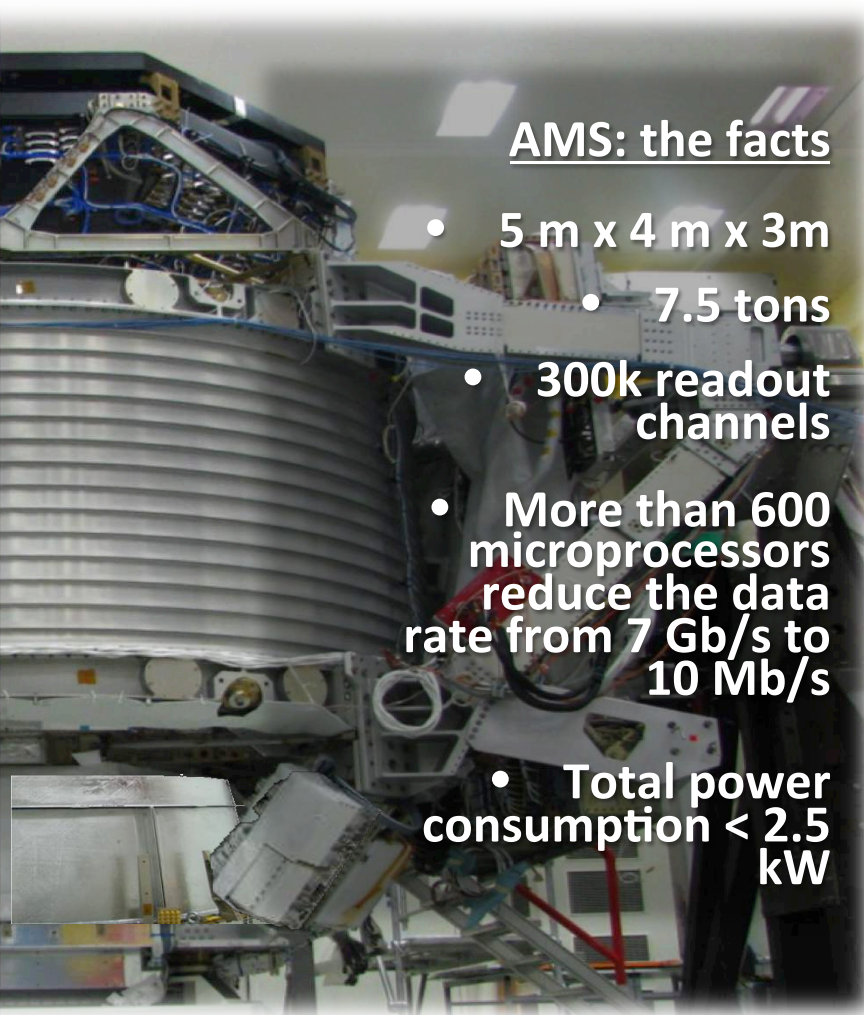
The high statistics of AMS required extensive studies of the systematic errors. Many cross-checks, several independent analyses.

This measurement provides the baseline for time variation studies: long-term solar modulation effects and SEP studies.



- The high precision of the measurements allow a detailed study of the variation of the fluxes spectral indices with rigidity
- The spectral index of both the proton and the helium flux increases at high rigidities, i.e. the fluxes cannot be described by a single power law
- The magnitude of the helium spectral index is different from that of the protons, but the rigidity dependence is similar.
- The spectral index of the p/He ratio above ~45 GV becomes constant: the high-rigidity p/He ratio is well described by a single power law

The Instrument – Pre-launch Integration

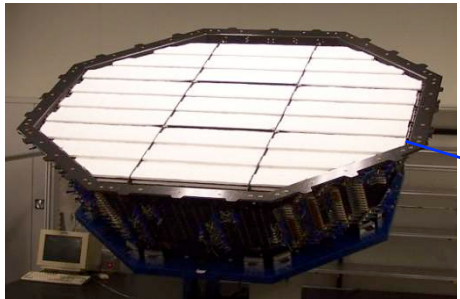


The AMS-02 instrument



TRD

Identify e^+ , e^-



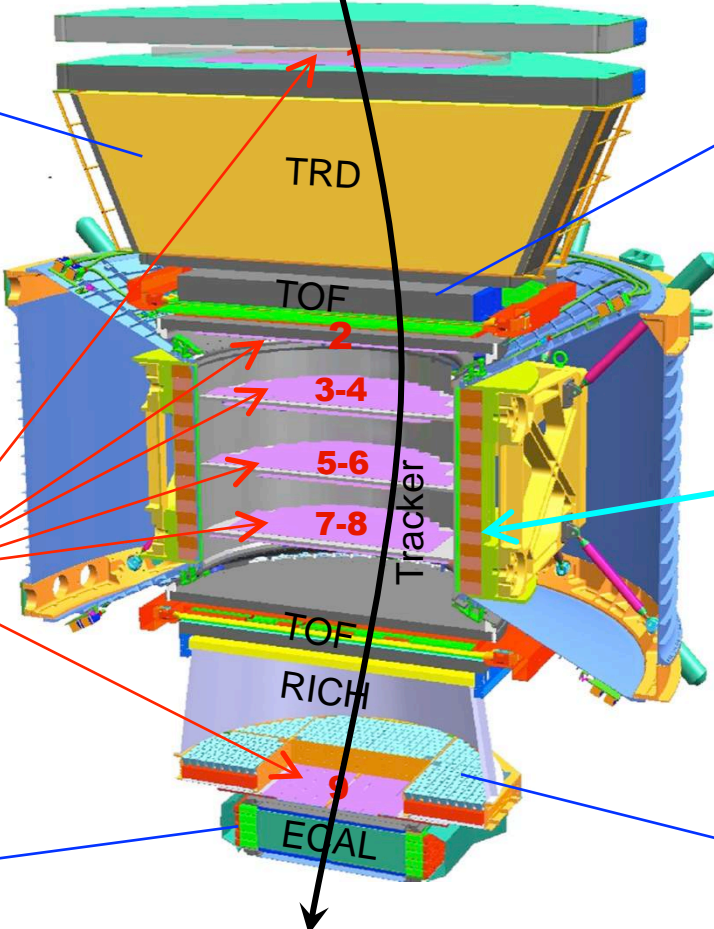
Silicon Tracker
 Z, P



ECAL
 E of e^+ , e^- , γ



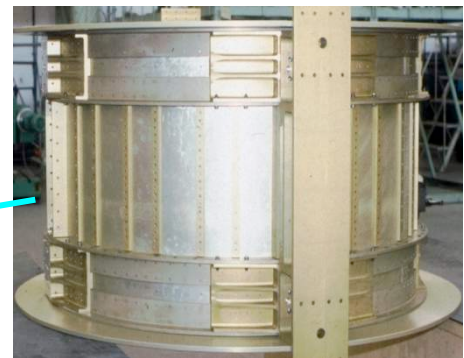
Particles and nuclei are defined by their charge (Z) and energy ($E \sim P$)



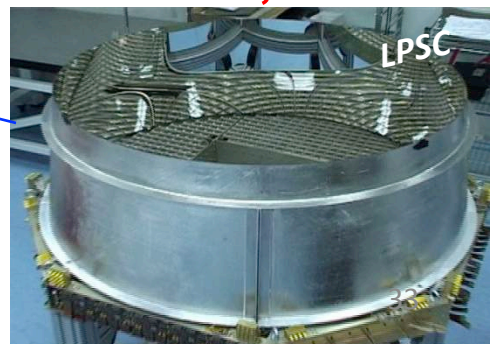
TOF
 Z, E



Magnet
 $+Z$



RICH
 Z, E

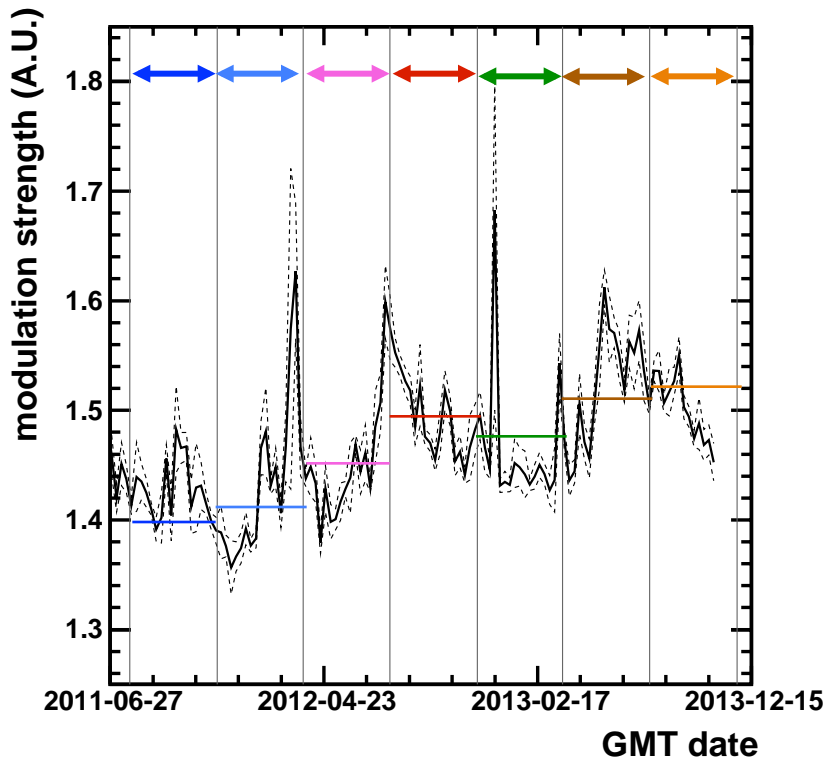
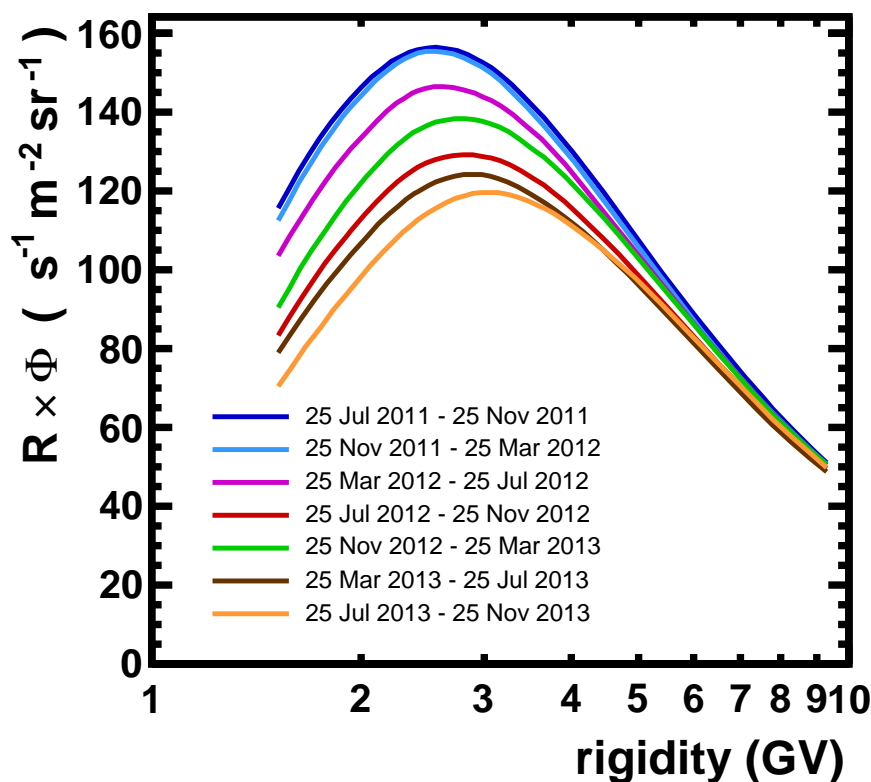


Z, P are measured independently from Tracker, RICH, TOF and ECAL

Low-Energy He spectrum and solar modulation

Helium spectrum from AMS data

Modulation strength from neutron monitor data (OULU station)



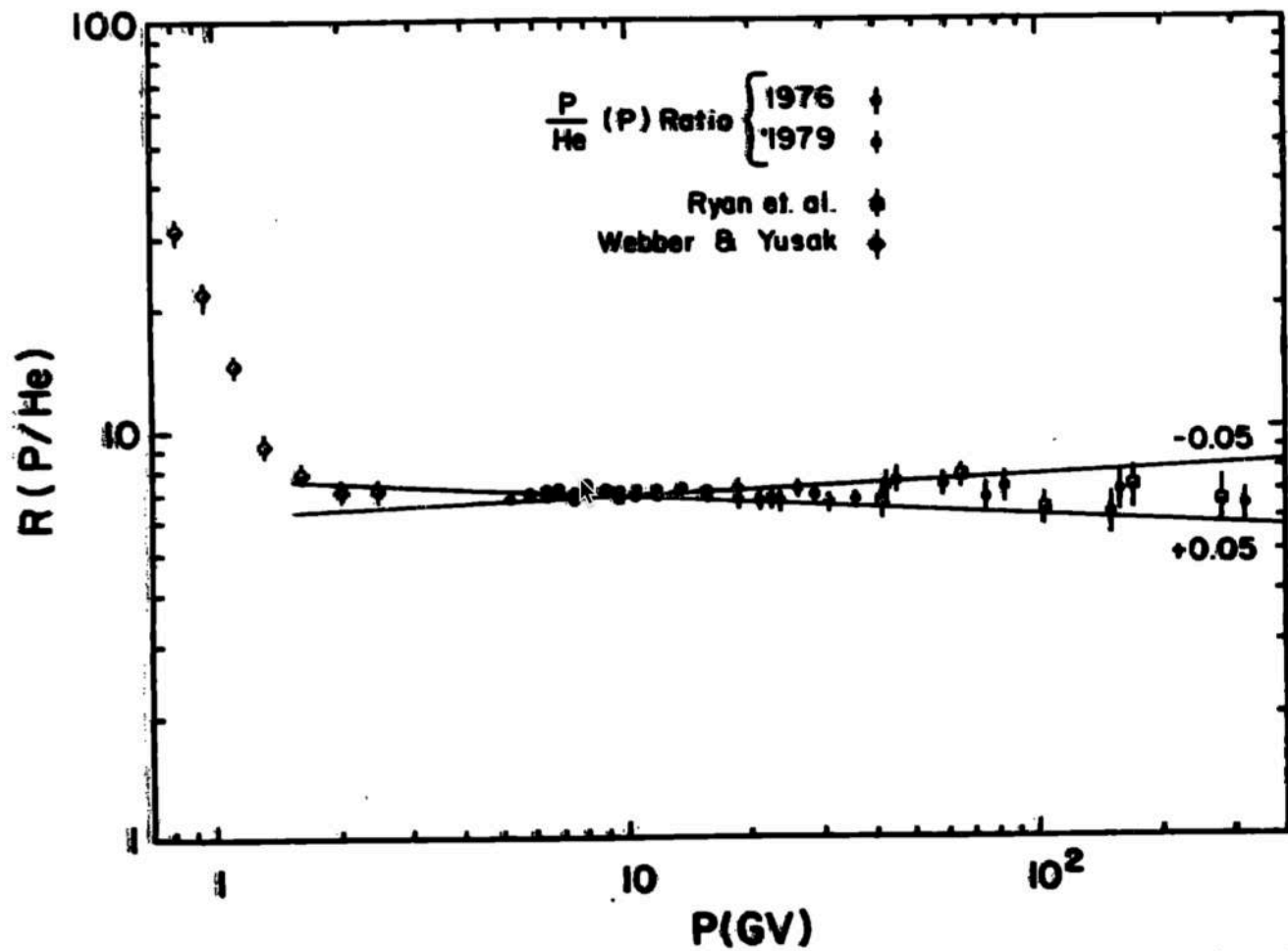
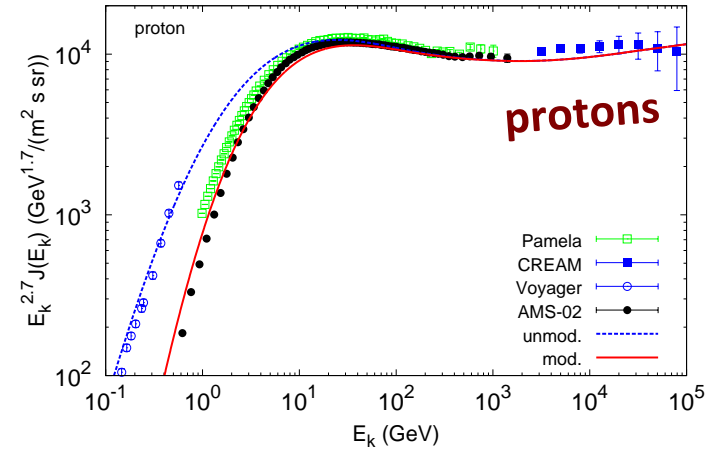


Figure 3. Proton to Helium ratio as a function of rigidity.

R. Webber et al. 1972

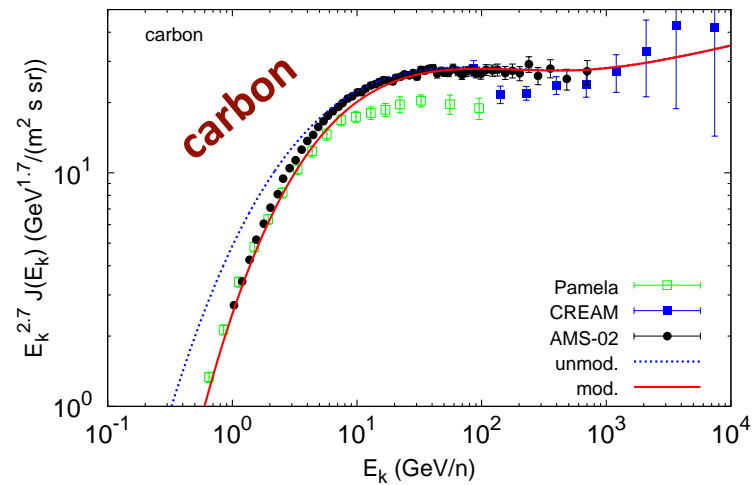
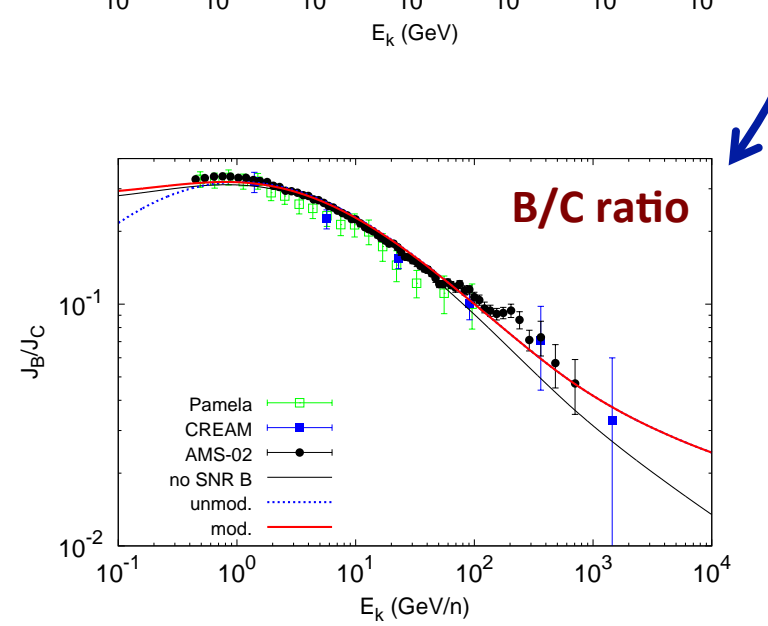
New phenomena in cosmic-ray propagation?

Non-linear CR transport due to self-induced turbulence



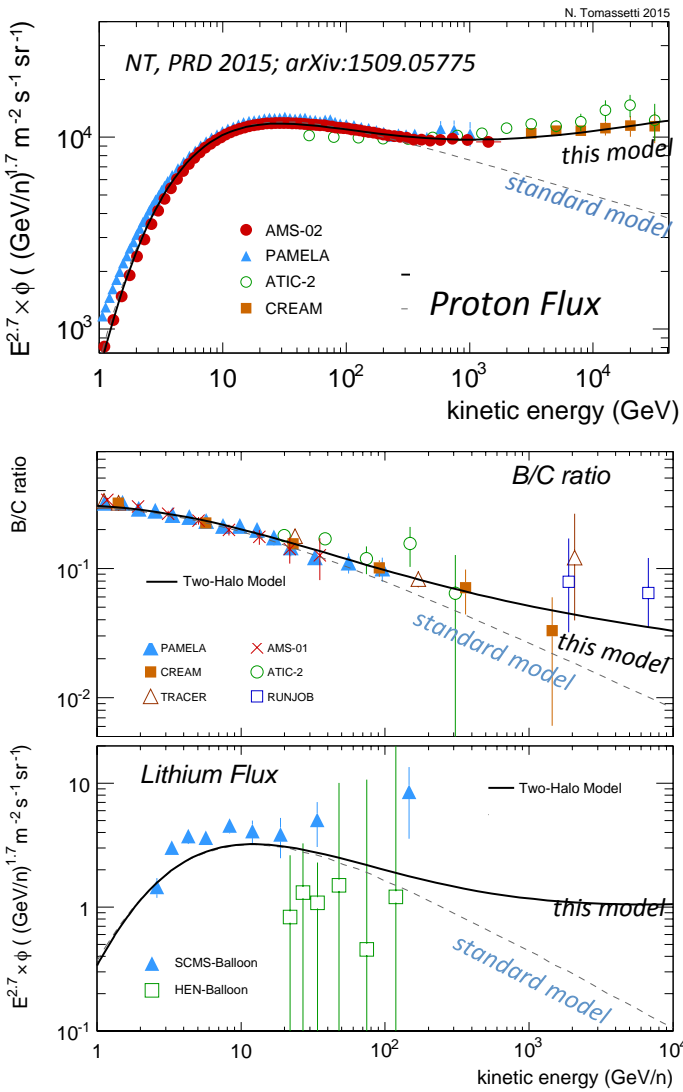
R. Aloisio et al. 1507.00594; P. Blasi et al. 1207.3706

- Diffusion to CR-induced turbulence at $E \sim 1\text{-}300 \text{ GeV}$
- Advection to CR-generated Alfvèn waves at $E < 1 \text{ GeV}$
- Diffusion to pre-existing turbulence at $> 300 \text{ GeV}$
- ✓ Flattening in all nuclei and sec/pri ratios
- ✓ Low energy Voyager-1 data.
- ✓ B/C seems to require an additional primary component



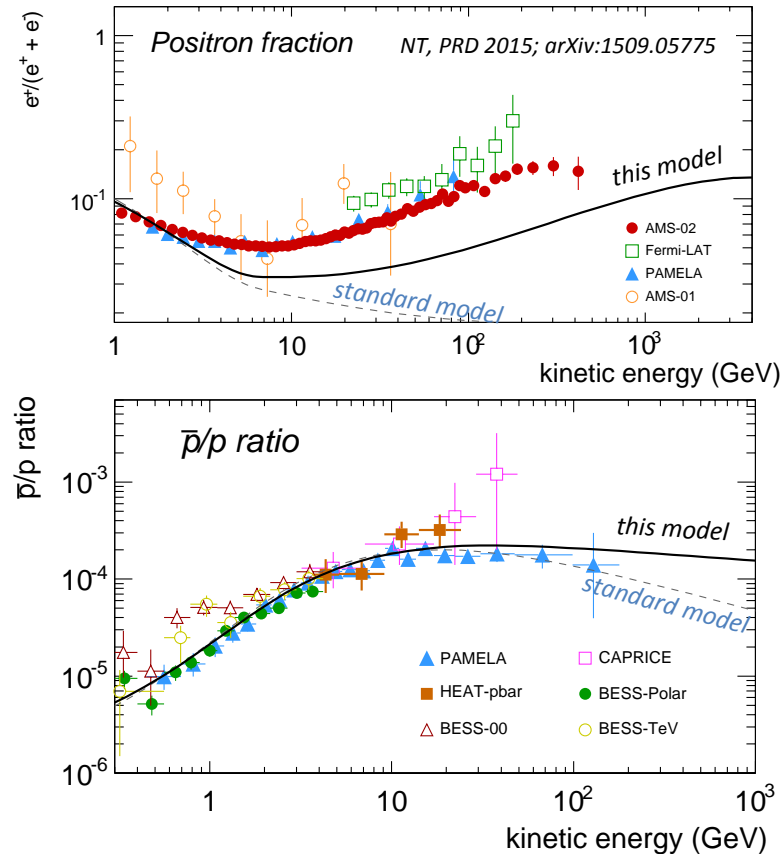
New phenomena in cosmic-ray propagation?

Diffusion coefficient is not separable into energy and space coordinates → no power-law
Shallower diffusivity in the region close to the Galactic disk → high-energy flattening



NT, 1204.4492 (2012); NT, 1509.05775 (2015)

- ✓ Predicted flattening in all nuclei and sec/pri ratios
- ✓ Enhanced antimatter production at high energy
- ✓ Connection with gamma-rays and anisotropy

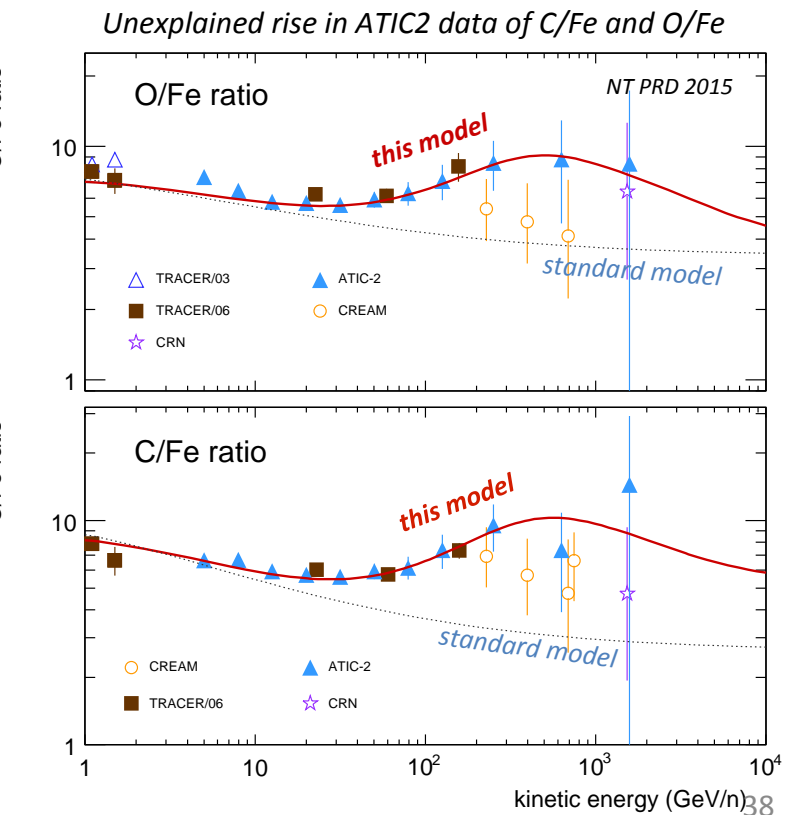
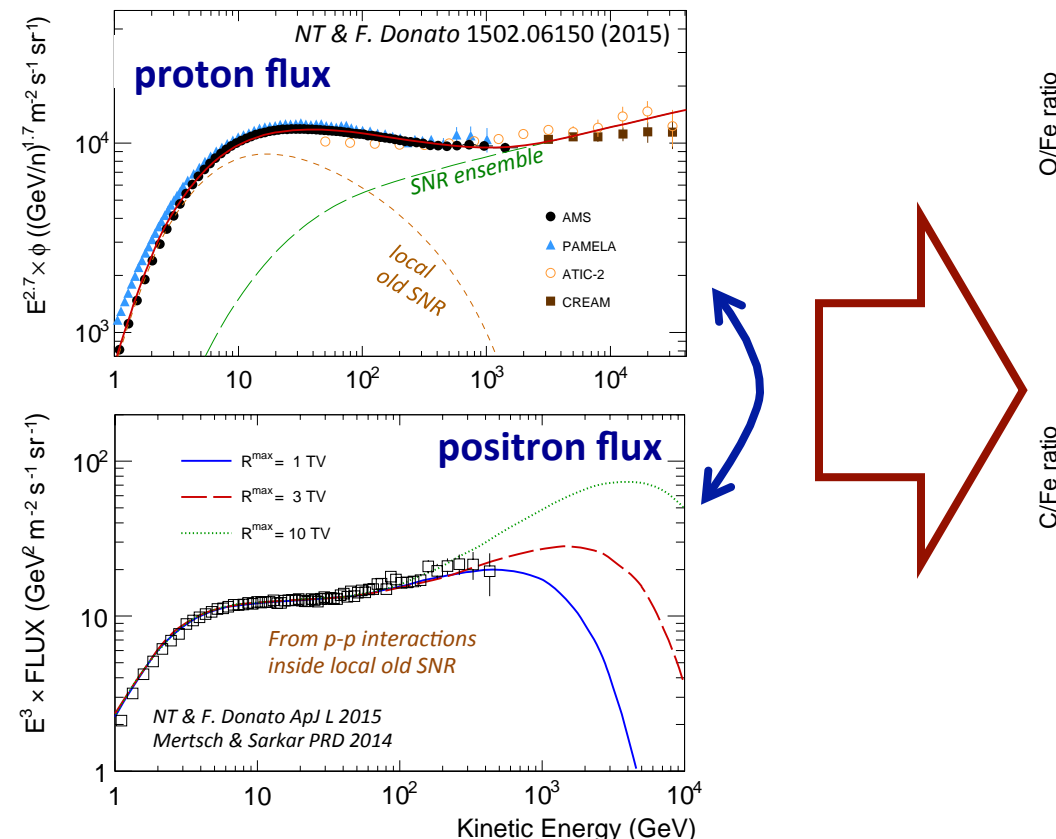


New [nearby-SNR] components in the CR spectrum?

two SNR components in the CR flux

- *Nearby source component for the GeV-TeV flux (and e^+ excess)*
Must have $R_{max} \sim TeV$ and secondary production ($B \sim 1uG$, $n > n_{ISM}$, $v \sim 10^7 cm/s \rightarrow OLD\ SNR$)
- *Galactic SNR ensemble*
Must have $R_{max} \sim PeV$: $B \sim 500uG$, $v \sim 10^9 m/s \rightarrow YOUNG\ SNRs$

- ✓ Connection between hadron spectra and positron excess [NT & F.Donato, 1502.06150 (2015)]
- ✓ Predicted features in heavy nuclei: explanation of C/Fe and O/Fe [NT, 1509.05774 (2015)]
- ✓ Connection with p/He ratio anomaly? [NT in preparation] [Kachelriess et al. 1504.06472 (2015)]



AMS Hadronic Tomography

with the cosmic-ray p/He ratio

Exposure Time: May 20 2011 – May 20 2012

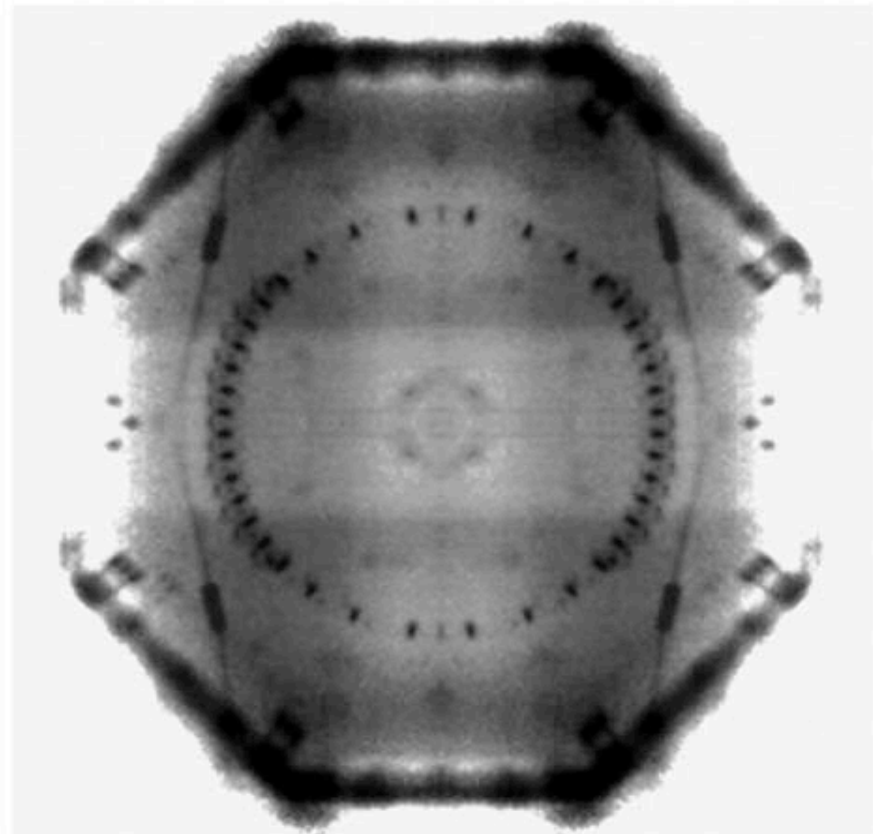
Number of Protons: 3,676,863,217

Number of Helium nuclei: 620,303,906

Rigidity range: 2 GV – 2000 GV

Tomographic plane: Z = +165 cm

XY pixel area: 1 cm²



Tomographic reconstruction of the AMS top-of-instrument material obtained using the Proton-to-Helium flux ratio. Tiny differences in the interaction cross-section of proton and He are used to trace the material inhomogeneities. Several detector elements such as screws, electronics boards, and mechanical interfaces are clearly recognizable.